Platinum-Catalyzed Asymmetric Alkylation of a Secondary Phosphine: Mechanism and Origin of Enantioselectivity

Corina Scriban,[†] David S. Glueck,*[,†] James A. Golen,[‡] and Arnold L. Rheingold[‡]

Departments of Chemistry, 6128 Burke Laboratory, Dartmouth College, Hanover, New Hampshire 03755, and University of California, San Diego, 9500 Gilman Drive, La Jolla, California 92093

Received December 8, 2006

The catalyst precursor Pt((*R*,*R*)-Me-Duphos)(Ph)(Cl) (**1**) mediated asymmetric alkylation of the secondary phosphine PHMe(Is) (**2**; Is = 2,4,6-(*i*-Pr)$_3$C$_6$H$_2$) with benzyl bromide in the presence of the base NaOSiMe$_3$ to yield enantioenriched PMeIs(CH$_2$Ph) (**3**). A mechanism for the catalysis has been proposed, on the basis of studies of the individual stoichiometric steps. The terminal phosphido complex Pt((*R*,*R*)-Me-Duphos)(Ph)(PMeIs) (**4**) was formed by proton transfer from **2** to the silanolate ligand in Pt((*R*,*R*)-Me-Duphos)(Ph)(OSiMe$_3$) (**5**), which was generated from **1** (or from Pt((*R*,*R*)-Me-Duphos)(Ph)(Br) (**7**)) and NaOSiMe$_3$. The silanolate complex **5** reacted with water to yield Pt((*R*,*R*)-Me-Duphos)(Ph)(OH) (**6**); both **6** and **7** were crystallographically characterized. The stoichiometric reaction of **4** and benzyl bromide in toluene gave the bromide **7** and **3**. In more polar solvents these compounds were in equilibrium with the cation [Pt((*R*,*R*)-Me-Duphos)(Ph)(PMeIs(CH$_2$Ph))][Br] (**8-Br**), the major Pt complex present during catalysis, which was isolated as the BF$_4$ salt. Treatment of **8-BF$_4$** with **2** and NaOSiMe$_3$ yielded phosphine **3** and regenerated phosphido complex **4**. This reaction does not appear to proceed via phosphine ligand substitution on **8-BF$_4$** to yield the secondary phosphine complex cation [Pt((*R*,*R*)-Me-Duphos)(Ph)(PHMe(Is))][BF$_4$] (**12**). Instead, treatment of **8-BF$_4$** with NaOSiMe$_3$ gave phosphine **3** and **5**, which then reacted with **2** to yield **4**. The crystal structure of the major diastereomer of **8-BF$_4$** showed that the major enantiomer of **3** formed by catalyst precursor **1** had an R_P absolute configuration. Low-temperature NMR studies on the major diastereomer of phosphido complex **4** were consistent with the R_P solid-state structure. Thus, the major enantiomer of phosphine **3** appeared to be formed from the major diastereomer of intermediate **4**, and enantioselectivity was determined mainly by the thermodynamic preference for one of the rapidly interconverting diastereomers of **4**, although their relative rates of alkylation were also important (Curtin−Hammett kinetics).

Introduction

We recently reported a new method for asymmetric synthesis of P-stereogenic phosphines: Pt-catalyzed asymmetric alkylation of racemic secondary phosphines.[1] Independently, Bergman and co-workers developed a similar Ru-catalyzed process.[2] Our work was guided by the hypothesis shown in Scheme 1. Terminal metal phosphido complexes undergo rapid phosphorus inversion.[3] With a chiral ancillary ligand, the diastereomers $\mathbf{A_R}$ and $\mathbf{A_S}$ of a P-stereogenic phosphido complex (*[M]−PRR′) often interconvert quickly on the NMR time scale;[4] they are nucleophilic[5] and react with electrophiles, such as alkyl halides, with different rate constants k_R and k_S to make new P−C bonds. If the interconversion of $\mathbf{A_R}$ and $\mathbf{A_S}$ is faster than their alkylation (k_1, $k_{-1} \gg k_R$, k_S), then the product ratio $P = [\mathbf{R}]/[\mathbf{S}]$ will be given by $P = K_{eq}[k_R/k_S]$ (Curtin−Hammett kinetics).[6,7]

Scheme 1. Phosphorus Inversion and Alkylation in Diastereomeric Metal Phosphido Complexes[a]

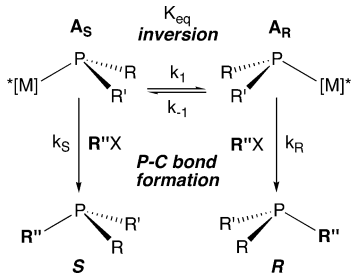

[a] M* = chiral metal−ligand fragment, R″X = alkyl halide.

For enantioselective catalysis to succeed, the background reaction of a secondary phosphine with an electrophile must be much slower than the metal-catalyzed reaction, and the chiral ancillary ligand must resist displacement from the metal by the excess phosphine substrate and products. To meet these requirements, we used the base NaOSiMe$_3$ to minimize the concentra-

* To whom correspondence should be addressed. E-mail: Glueck@Dartmouth.Edu.

[†] Dartmouth College.

[‡] University of California, San Diego.

(1) Scriban, C.; Glueck, D. S. *J. Am. Chem. Soc.* **2006**, *128*, 2788−2789.

(2) Chan, V. S.; Stewart, I. C.; Bergman, R. G.; Toste, F. D. *J. Am. Chem. Soc.* **2006**, *128*, 2786−2787.

(3) Rogers, J. R.; Wagner, T. P. S.; Marynick, D. S. *Inorg. Chem.* **1994**, *33*, 3104−3110.

(4) (a) Wicht, D. K.; Kovacik, I.; Glueck, D. S.; Liable-Sands, L. M.; Incarvito, C. D.; Rheingold, A. L. *Organometallics* **1999**, *18*, 5141−5151. (b) Moncarz, J. R.; Laritcheva, N. F.; Glueck, D. S. *J. Am. Chem. Soc.* **2002**, *124*, 13356−13357.

(5) (a) Malisch, W.; Maisch, R.; Colquhoun, I. J.; McFarlane, W. *J. Organomet. Chem.* **1981**, *220*, C1−C6. (b) Bohle, D. S.; Jones, T. C.; Rickard, C. E. F.; Roper, W. R. *Organometallics* **1986**, *5*, 1612−1619. (c) Crisp, G. T.; Salem, G.; Wild, S. B.; Stephens, F. S. *Organometallics* **1989**, *8*, 2360−2367. (d) Buhro, W. E.; Zwick, B. D.; Georgiou, S.; Hutchinson, J. P.; Gladysz, J. A. *J. Am. Chem. Soc.* **1988**, *110*, 2427−2439.

(6) Seeman, J. R. *Chem. Rev.* **1983**, *83*, 83−134.

(7) For an example of Scheme 1 in the alkylation of a chiral Fe−phosphido complex, see ref 5c.

10.1021/om061116s CCC: $37.00
Publication on Web 02/20/2007

Scheme 2[a]

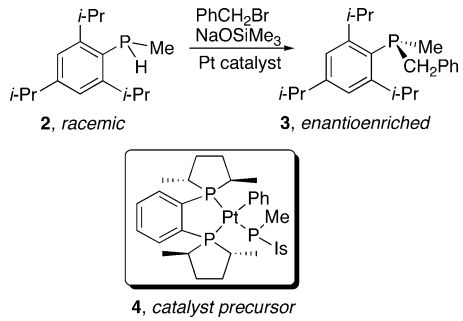

[a] Is = 2,4,6-(*i*-Pr)$_3$C$_6$H$_2$.

Scheme 3[a]

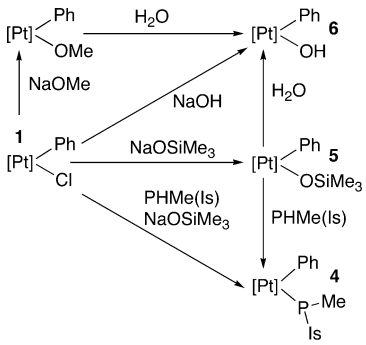

[a] [Pt] = Pt((*R*,*R*)-Me-Duphos).

tion of the phosphido anion [PRR′]$^-$ and the rigid bidentate chiral alkylphosphine (*R*,*R*)-Me-Duphos to ensure tight binding to the metal. We chose the secondary phosphine substrate PHMe(Is) (**2**; Is = 2,4,6-(*i*-Pr)$_3$C$_6$H$_2$),[8] with a large Is and a small Me substituent, in hopes of controlling the equilibrium ratio of phosphido diastereomers (K_{eq}; Scheme 1). Indeed, Pt-catalyzed alkylation of **2** was enantioselective (77% ee; Scheme 2).[1]

To test the hypothesis of Scheme 1, we studied the mechanism of this catalytic reaction in detail by investigating the stoichiometric steps leading to P−C bond formation, the possibility of catalyst inhibition by strong binding of the product phosphine, and the origin of enantioselectivity.

Results and Discussion

1. Synthesis and Structure of Potential Intermediates in Catalysis. (a) Formation of Phosphido Complex 4. The catalyst precursor Pt((*R*,*R*)-Me-Duphos)(Ph)(PMeIs) (**4**)[1] was prepared by treating Pt((*R*,*R*)-Me-Duphos)(Ph)(Cl) (**1**)[9] with PHMe(Is)/NaOSiMe$_3$ (Scheme 3); air-stable **1** was a more convenient and general precatalyst. Reaction of **1** with NaOSiMe$_3$ generated the silanolate Pt((*R*,*R*)-Me-Duphos)(Ph)(OSiMe$_3$) (**5**), which was characterized spectroscopically. We could not isolate **5** in pure form because of its ready reaction with traces of water to yield the hydroxide complex Pt((*R*,*R*)-Me-Duphos)(Ph)(OH) (**6**), which was prepared independently from chloride **1** and NaOH, or from the methoxide Pt((*R*,*R*)-Me-Duphos)(Ph)(OMe) and water (Scheme 3 and the Supporting Information).[10] Hydroxide **6** was structurally characterized by X-ray crystallography (see Figure 1, Table 1, and the Supporting Information for details).

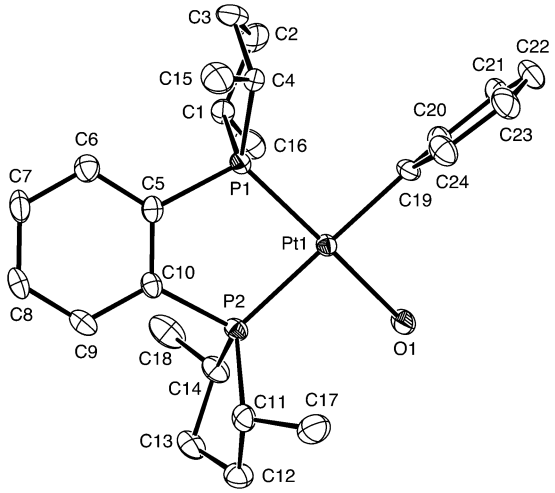

Figure 1. ORTEP diagram of Pt((*R*,*R*)-Me-Duphos)(Ph)(OH) (**6**), showing one of the two independent molecules in the asymmetric unit.

Table 1. Crystallographic Data for the Complexes Pt((*R*,*R*)-Me-Duphos)(Ph)(X) (X = OH (6), Br (7), PMeIs(CH$_2$Ph) (8-BF$_4$))[a]

	6	**7**	**8-BF$_4$**
formula	$C_{24}H_{34}OP_2Pt$	$C_{24}H_{33}BrP_2Pt$	$C_{47}H_{66}BF_4P_3Pt$
formula wt	595.54	658.44	1005.81
space group	$P2_1$	$P2_12_12_1$	$P2_12_12_1$
a, Å	8.434(2)	10.701(2)	12.9514(16)
b, Å	13.588(4)	13.890(3)	17.462(2)
c, Å	20.825(6)	16.873(3)	21.291(3)
α, deg	90	90	90
β, deg	101.266(6)	90	90
γ, deg	90	90	90
V, Å^3	2340.7(11)	2508.0(8)	4814.9(10)
Z	4	4	4
D(calcd), g/cm^3	1.690	1.744	1.388
μ(Mo Kα), mm^{-1}	6.143	7.323	3.059
temp, K	208(2)	213(2)	213(2)
$R(F)$, %[b]	4.48	2.36	2.27
$R_w(F^2)$, %[b]	10.02	4.94	4.94

[a] Complexes **6** and **7** are neutral; **8** is a cation (BF_4 anion). [b] Quantity minimized: $R_w(F^2) = \sum[w(F_o^2 - F_c^2)^2]/\sum[(wF_o^2)^2]^{1/2}$; $R = \sum\Delta/\sum(F_o)$, $\Delta = |(F_o - F_c)|$, $w = 1/[\sigma^2(F_o^2) + (aP)^2 + bP]$, $P = [2F_c^2 + \mathrm{Max}(F_o^2,0)]/3$. A Bruker CCD diffractometer was used in all cases.

The silanolate **5** reacted quickly with PHMe(Is) (Scheme 3) to yield the phosphido complex **4**, which was expected to exist as a mixture of two diastereomers, rapidly interconverting by P inversion. At room temperature, only one set of NMR signals for this complex was observed, consistent with the predicted behavior. As discussed in more detail elsewhere, four diastereomers of **4** were observed by low-temperature ^{31}P NMR spectroscopy in a 98:1:1:2 ratio at −50 °C.[11] The "extra" signals appeared to include some rotamers of the expected two "invertomers". We could not directly measure the barrier to inversion in **4**, but barriers in the closely related complexes Pt((*R*,*R*)-*i*-Pr-Duphos)(Ph)(PMeIs) and Pt((*R*,*R*)-Me-Duphos)(X)-

(8) Brauer, D. J.; Bitterer, F.; Dorrenbach, F.; Hessler, G.; Stelzer, O.; Kruger, C.; Lutz, F. *Z. Naturforsch., B* **1996**, *51*, 1183−1196.

(9) Brunker, T. J.; Blank, N. F.; Moncarz, J. R.; Scriban, C.; Anderson, B. J.; Glueck, D. S.; Zakharov, L. N.; Golen, J. A.; Sommer, R. D.; Incarvito, C. D.; Rheingold, A. L. *Organometallics* **2005**, *24*, 2730−2746.

(10) For related platinum alkoxides and hydroxides and their interconversion, see: (a) Appleton, T. G.; Bennett, M. A. *Inorg. Chem.* **1978**, *17*, 738−747. (b) Bryndza, H. E.; Calabrese, J. C.; Wreford, S. S. *Organometallics* **1984**, *3*, 1603−1604. (c) Bryndza, H. E.; Fong, L. K.; Paciello, R. A.; Tam, W.; Bercaw, J. E. *J. Am. Chem. Soc.* **1987**, *109*, 1444−1456.

(11) Scriban, C.; Glueck, D. S.; DiPasquale, A. G.; Rheingold, A. L. *Organometallics* **2006**, *25*, 5435−5448.

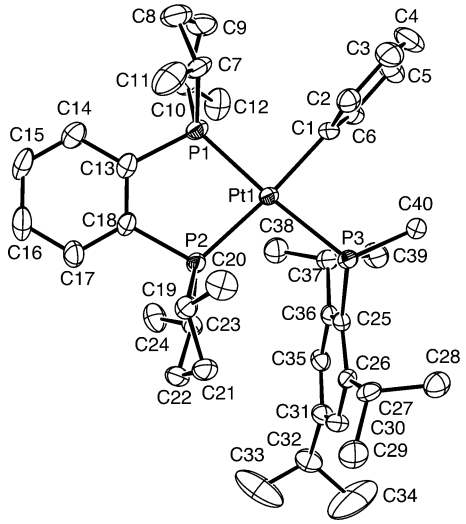

Figure 2. ORTEP diagram of Pt((*R*,*R*)-Me-Duphos)(Ph)(PMeIs) (**4**).[11]

Chart 1. Possible Phosphido Configurations in the Major Diastereomer of 4, with Solid-State Models

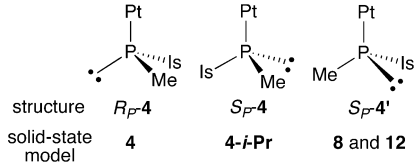

(PMeIs) (X = Cl, I) were about 10−12 kcal/mol,[11] similar to those in related phosphido complexes cited in refs 3 and 11.

In the solid state only one diastereomer of **4**, with an (R_P)-PMeIs group, was observed in the crystal studied (Figure 2).[11] The related complexes Pt((*R*,*R*)-Me-Duphos)(X)(PMeIs) (X = I, Cl, PMeIs) also crystallized with the R_P configuration, while Pt((*R*,*R*)-*i*-Pr-Duphos)(Ph)(PMeIs), whose Duphos ligand has an absolute configuration *opposite* that of the (*R*,*R*)-Me-Duphos one, crystallized as the S_P diastereomer.[11] The simplest explanation of these observations is that the R_P configuration was thermodynamically favorable for the (*R*,*R*)-Me-Duphos complexes and the major diastereomer was observed in each case. However, it is also possible that this diastereomer was favored in the solid state or that the crystals chosen for structure determination were not representative of the bulk.

Therefore, we used low-temperature NMR spectroscopy to investigate the absolute configuration of the major diastereomer of **4** in solution; details are given in the Experimental Section and the Supporting Information.[12] Rotation about the Pt−C(Ph) bond was slow under these conditions, and the known (*R*,*R*)-Me-Duphos stereochemistry was used to determine the position of the Pt−Ph group, which appeared to be perpendicular to the square plane, as in the solid state (Figure 2). ^{1}H−^{1}H NOEs between the cis (P1) phospholane substituents and the Pt−Ph hydrogens were then used to establish the relative position of the Pt−Ph group with respect to the square plane (H2 and H3 above, H5 and H6 below).

This information on the structure and conformation of the Pt((*R*,*R*)-Me-Duphos)(Ph) fragment was then used to investigate the absolute configuration of the phosphido ligand. Chart 1 shows three different ways to arrange the Me, Is, and Pt substituents and the lone pair about the pyramidal P center. (R_P)-**4** corresponds to the solid-state structure (Figure 2). The opposite stereochemistry ((S_P)-**4**) was observed in the crystal structure of **4-*i*-Pr**.[11] Finally, rotation of (S_P)-**4** about the Pt−P bond would yield the diastereomer (S_P)-**4′**, which is related to the solid-state structures of the cations [Pt((*R*,*R*)-Me-Duphos)(Ph)(PMeIs(CH_2Ph))][BF_4] (**8**; see below) and [Pt((*R*,*R*)-Me-Duphos)(Ph)(PHMe(Is))][BF_4] (**12**).[11]

NOEs between the PMeIs group and the Pt((*R*,*R*)-Me-Duphos)(Ph) fragment were used to differentiate these structures. First, several P−Me to Pt−Ph NOEs were observed (Figure 3), but since the PMe (C40) and Duphos Me (C11) ^{1}H NMR signals overlapped, assignment was not straightforward. However, estimating the H−H distances (Pt−Ph to P−Me and Pt−Ph to Duphos Me) from the crystal structure of (R_P)-**4** enabled assignment of NOEs to one or both of the methyl groups (Table 2, Figure 3).

These observations, as well as NOEs observed between Is hydrogens and the Pt−Ph group and substituents on both phospholane rings, were consistent with the solid-state structure and the (R_P)-PMeIs absolute configuration (Supporting Information). Ideally, determination of the solution structures of *both* diastereomers of **4**, and comparison of the data, would enable definitive assignment of the absolute configuration. However, because of the thermodynamic bias for one diastereomer of **4**, presumed to have the R_P configuration, detailed NMR studies of the minor isomer ((S_P)-**4** or (S_P)-**4′**) were not possible.[13]

The crystal structure of (S_P)-Pt((*R*,*R*)-*i*-Pr-Duphos)(Ph)(PMeIs) (**4-*i*-Pr**) provided a model for (S_P)-**4**.[11] The Pt(Ph)(PMeIs) fragments in the solid-state structures of **4** and **4-*i*-Pr** adopted similar conformations. As a result of the opposite absolute configurations, however, the PMeIs group was found on different sides of the Pt−Ph ring in **4** and **4-*i*-Pr** (Figure 4). The position of the P−Me groups (C40 and C1, respectively) changed little in these structures; the estimated P−Me to Pt−Ph H−H distances calculated using **4-*i*-Pr** as a model for (S_P)-**4** (as in Table 2; see the Supporting Information, Table S3) were also consistent with the observed NOEs.

However, the positions of the P−Is groups differed significantly in **4** and **4-*i*-Pr** (Figure 4). Although the argument requires several assumptions, a combination of the estimated H−H distances between the *o*-*i*-Pr methine hydrogens H37 (in **4**) and H8 (in **4-*i*-Pr**) and the Pt−Ph ring (Table 3) and the NOE observations may be used to differentiate structures **4** and **4-*i*-Pr** and the associated P stereochemistries.

The observed NOEs for **4** from H37 to H6 and H5 (Figure 4) were consistent with the estimated solid-state distances, highlighted in boldface type in Table 3. The hypothetical (S_P)-**4** (if **4-*i*-Pr** is a good model for it) would be expected to show NOEs from H37 to H2, H3, and H6 but not to H4 and H5 (Table 3, highlighted in boldface type for H8, the analogue of H37 in **4-*i*-Pr**). Although it is dangerous to make arguments on the basis of negative observations,[14] the lack of NOEs between H37 and H2 or H3, combined with the observed H37−H5 NOE, is consistent with (R_P)-**4** and not with (S_P)-**4** (as modeled by (S_P)-**4-*i*-Pr**).

It is difficult to rule out another possible structure ((S_P)-**4′**), derived from (R_P)-**4** by interchanging the P−Me and the lone pair, which would require minimal motion and be consistent with observed NOEs to the Is group (Figure 4). However,

(12) For a related report of NOESY data for Pd(Me-Duphos) aryl complexes, see: Drago, D.; Pregosin, P. S. *Organometallics* **2002**, *21*, 1208−1215.

(13) As described in more detail above and in ref 11, four diastereomers of **4** were observed at low temperature; we were only able to study the NMR spectra of the major one in detail.

(14) Neuhaus, D.; Williamson, M. P. *The Nuclear Overhauser Effect in Structural and Conformational Analysis.* VCH: New York, 1989; p 358.

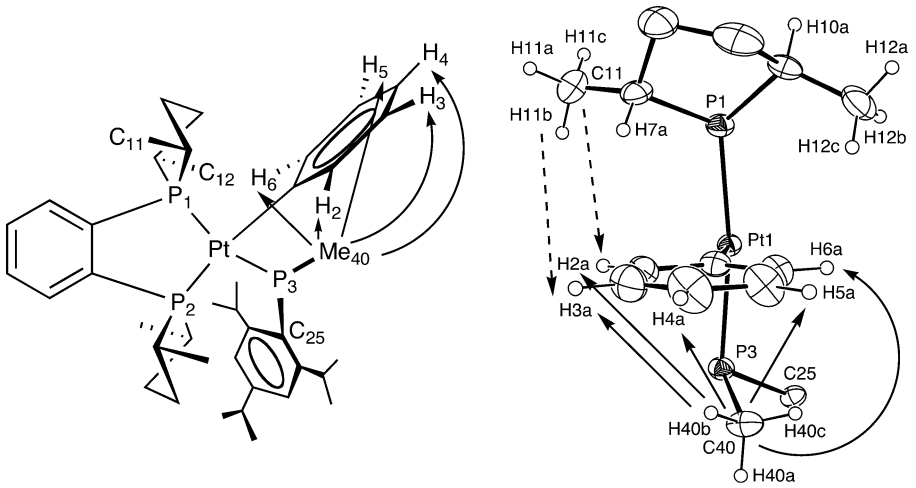

Figure 3. NOEs between the C40 P−Me group, the Duphos C11 Me group, and the Pt−Ph hydrogens and resulting assignments. For clarity, NOEs from the C11 Me group to the Pt−Ph hydrogens are not shown in the left-hand panel (see the related discussion in the text). Arrows in the right-hand panel (a portion of the ORTEP diagram in Figure 2) show NOEs from both the P−Me (C40, solid arrows) and the C11 Me (dashed arrows) to H2 and H3. As discussed above, however, we cannot tell which of the two methyl groups makes a bigger contribution to these NOEs.

Table 2. Calculated Average Distances (Å) between the Pt−Ph Hydrogens and the P−Me (C40) and Duphos Me (C11) Hydrogens in the Structure of 4 and the Resulting Assignment of the Observed Pt−Ph/Me NOEs

	d(H−H)		
Pt−Ph H	P−Me (C40) (av)	CHMe (C11) (av)	NOE assignt
H2a (o)	4.099	4.001	both
H3a (m)	4.851	5.583	both
H4a (p)	5.053	7.168	P−Me
H5a (m)	4.400	7.547	P−Me
H6a (o)	3.532	6.495	P−Me

comparison to the crystal structures of analogous complexes provided some evidence against this structure. Table 3 includes estimated H−C distances from the Pt−Ph hydrogens to the P−C carbons in **4** and **4-*i*-Pr**. The position of Is ipso carbon C2 in **4-*i*-Pr** is a model for the P−Me carbon in the hypothetical (S_P)-**4′** (Figure 4). The significantly longer estimated distances to it, in comparison to those to the real Me group (C1), are potentially inconsistent with the NOE observations. A similar trend is apparent for the C40−H(Ph) and C25−H(Ph) distances in **4** (Table 3).

Similarly, Figure 5 shows portions of the solid-state structures of **4** and its protonated and alkylated analogues [Pt((*R*,*R*)-Me-Duphos)(Ph)(PHMe(Is))][BF_4] (**12**)[11] and [Pt((*R*,*R*)-Me-Duphos)-(Ph)(PMeIs(CH_2Ph))][BF_4] (**8**; see below). The P−H hydrogen (H3) in **12** provided another model for the position of the P−Me in the hypothetical (S_P)-**4′**. The calculated position of H3 was further from the Pt−Ph ring than was the P−Me carbon (C40; see Table S5 in the Supporting Information), potentially inconsistent with the observed NOEs of Figure 3. Rotation about the Pt−P bond in **8-BF_4** places the benzyl group (C34) in a position distinct from those of other P substituents in **4**, **4-*i*-Pr**, and **12**. Here too C34 was further from the Pt−Ph ring than the P−Me carbon (C41; see Table S6 in the Supporting Information).

Therefore, the NOEs shown in Figures 3 and 4 and the Supporting Information are most simply explained by assuming that the major diastereomer of complex **4** contained a (R_P)-PMeIs group in solution, as observed in the solid state. Although this conclusion is consistent with both the solution NMR data and comparison to the crystal structure of **4** and several of its analogues, the absence of NMR data for the (inaccessible) minor diastereomer makes it impossible to definitively rule out an S_P configuration for **4**. With this caveat in mind, we assume that the major diastereomer of **4** is R_P in the mechanistic analysis below.

(b) Alkylation of Phosphido Complex 4. Formation of 3, 7, and 8. The stoichiometric reaction of **4** with benzyl bromide in toluene gave the bromide complex Pt((*R*,*R*)-Me-Duphos)-(Ph)(Br) (**7**) and the phosphine PMeIs(CH_2Ph) (**3**) (Scheme 4). Consistent with the ideas of Scheme 1 and the observations in catalysis, isolated phosphine **3** was enantioenriched (70% ee at 21 °C, 79% ee at −5 °C).

The structure of bromide complex **7** was analogous to that of the previously reported chloride **1** and hydroxide **6** (see Figure 6, Tables 1 and 4, and the Supporting Information).[9] The identical Pt−P (trans to halide) distances of 2.2028(11) and 2.2012(7) Å for **7** and **1**, respectively, showed that Br and Cl have the same trans influence in these complexes. This is consistent with ^{31}P NMR data in toluene; J_{Pt-P} values for the Duphos P trans to halide were 3892 and 3893 Hz for **7** and **1**.[15] The Pt−P (trans to OH) distance in **6** of 2.195(2) Å (average value for the two molecules in the unit cell), along with the J_{Pt-P} value (3218 Hz), showed that the trans influence of hydroxide is similar to that of these halides.

When a mixture of bromide **7** and phosphine **3** was dissolved in CD_2Cl_2, an equilibrium with the cation [Pt((*R*,*R*)-Me-Duphos)(Ph)(PMeIs(CH_2Ph))][Br] (**8-Br**) was observed (Scheme 4). A similar mixture was obtained when phosphido complex **4** was generated from Pt((*R*,*R*)-Me-Duphos)(Ph)(Cl) (**1**) with PHMe(Is)/$NaOSiMe_3$ in situ and then alkylated. These results are consistent with formation of the cation **8-Br** at equilibrium favored by a more polar medium.[16]

Treatment of **1** with $AgBF_4$ in acetonitrile yielded [Pt((*R*,*R*)-Me-Duphos)(Ph)(NCMe)][BF_4], and subsequent reaction with PMeIsCH_2Ph (**3**) gave **8-BF_4**, isolated as a mixture of two diastereomers. Reaction of **8-BF_4** with excess tetraoctylammonium bromide ($NOct_4Br$) in toluene gave phosphine **3** and bromide **7**, consistent with the proposed equilibrium (Scheme

(15) Appleton, T. G.; Clark, H. C.; Manzer, L. E. *Coord. Chem. Rev.* **1973**, *10*, 335−422.

(16) This is consistent with the equilibrium observed in ref 4b between Pd((*R*,*R*)-Me-Duphos)(Ph)(I), PHMe(Is) and the cation [Pd((*R*,*R*)-Me-Duphos)(Ph)(PHMe(Is))][I], which favored the neutral iodo complex.

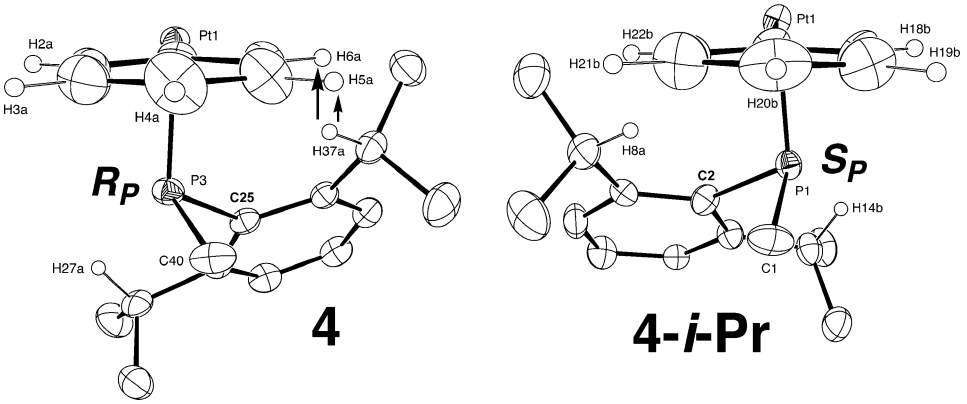

Figure 4. Partial ORTEP diagrams (*p*-*i*-Pr groups omitted) for the complexes (R_P)-Pt((*R*,*R*)-Me-Duphos)(Ph)(PMeIs) (**4**) and (S_P)-Pt-((*R*,*R*)-*i*-Pr-Duphos)(Ph)(PMeIs) (**4-*i*-Pr**, one of the two independent molecules in the unit cell), illustrating close contacts between ortho *i*-Pr CH groups H37 (in **4**) and H8 (in **4-*i*-Pr**) and the Pt−Ph ring. The arrows on the left show NOEs observed between *i*-Pr CH H37 and Pt−Ph hydrogens H5 and H6.

Table 3. Selected Estimated Solid-State H−H and H−C Distances (Å) in the Complexes (R_P)-Pt((*R*,*R*)-Me-Duphos)(Ph)(PMeIs) (4) and (S_P)-Pt((*R*,*R*)-*i*-Pr-Duphos)(Ph)(PMeIs) (4-*i*-Pr)[a]

Pt−Ph (**4**)	*d*(H−H) (H37)	*d*(C−H) (C40, Me)	*d*(C−H) (C25, Is)	Pt−Ph (**4-*i*-Pr**)	*d*(H−H) (H8)	*d*(C−H) (C1, Me)	*d*(C−H) (*C*2, Is)
H2a (o)	4.895	3.913	5.507	H22 (o)	**2.245**	3.607	4.643
H3a (m)	6.166	4.840	7.165	H21 (m)	**4.290**	4.669	6.515
H4a (p)	6.039	5.140	7.655	H20 (p)	5.860	5.190	7.598
H5a (m)	**4.495**	4.478	6.609	H19 (m)	6.037	4.764	7.178
H6a (o)	**2.393**	3.453	4.738	H18 (o)	**4.816**	3.754	5.546

[a] Distances were estimated using calculated hydrogen atom positions; average values for the two independent molecules are reported for **4-*i*-Pr**. Distances given in boldface type for **4** correspond to observed NOEs, while distances given in boldface type for **4-*i*-Pr** correspond to predicted NOEs.

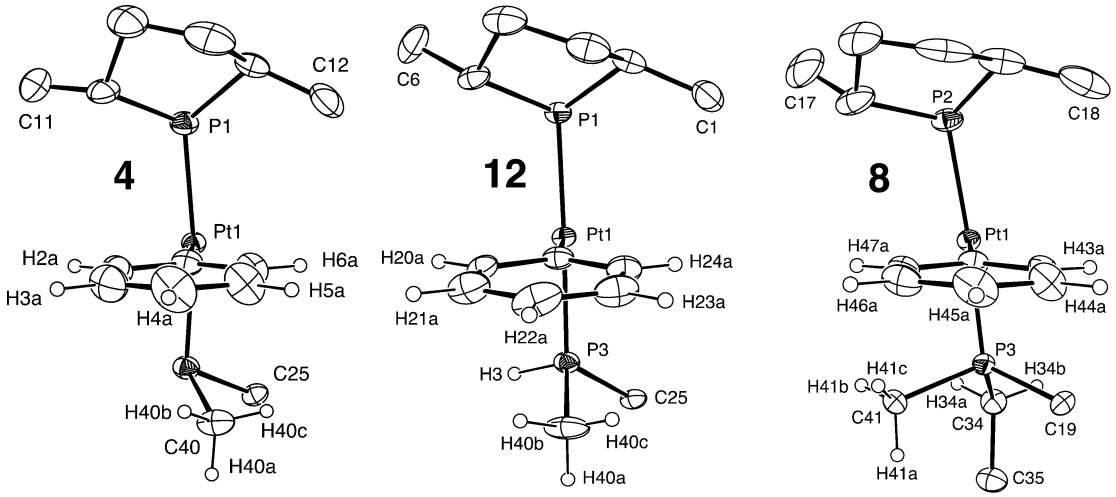

Figure 5. Partial ORTEP diagrams of the complexes Pt((*R*,*R*)-Me-Duphos)(Ph)(PMeIs) (**4**), [Pt((*R*,*R*)-Me-Duphos)(Ph)(PHMe(Is))][BF_4] (**12-BF_4**), and [Pt((*R*,*R*)-Me-Duphos)(Ph)(PMeIs(CH_2Ph))][BF_4] (**8-BF_4**).[11]

4). The crystal structure of the major diastereomer of **8-BF_4** (Figure 7, Table 1, and the Supporting Information) and the ^{1}H NMR spectrum of the single crystal used for structure determination showed that its coordinated phosphine had an S_P absolute configuration. This corresponds to the R_P configuration for the major enantiomer of phosphine **3**, without the Pt substituent.

Comparison of this structure with that of **4** and its protonated derivative [Pt((*R*,*R*)-Me-Duphos)(Ph)(PHMe(Is))][BF_4] (**12**) provided information on the structural consequences of protonation/alkylation at P (Table 5).[11] The sum of angles at P3 increased on quaternization, from 320.6(2)° in the phosphido species **4** (pyramidal geometry) to 342.47(19)° in the secondary phosphine complex **12** (reduced steric demand of a proton in comparison to the P lone pair). The average P3 angle in the alkylated cation **8-BF_4** was 109.43(15)°, the ideal value for tetrahedral geometry.

Scheme 4[a]

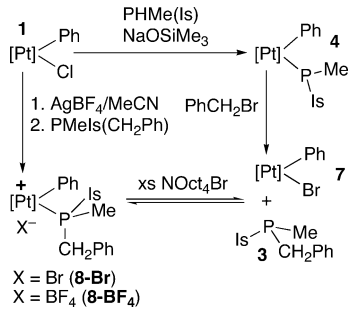

[a] [Pt] = Pt((*R*,*R*)-Me-Duphos).

Presumably P3 is more tetrahedral in **8-BF_4** than in **12** because the benzyl group is more sterically demanding than the proton. Even with the increased steric bulk around P, the Pt−P3 distance

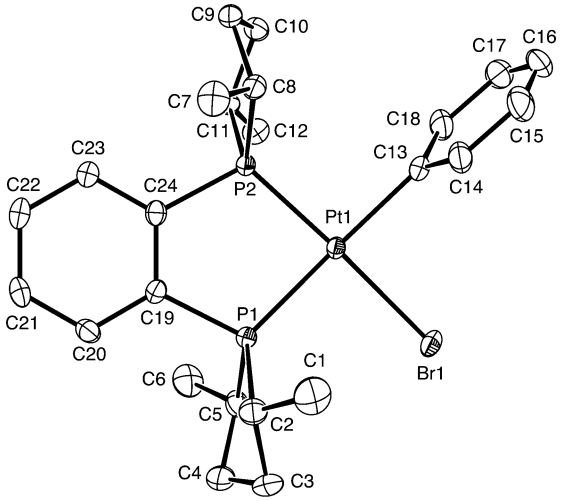

Figure 6. ORTEP diagram of Pt((*R*,*R*)-Me-Duphos)(Ph)(Br) (**7**).

Table 4. Selected Bond Lengths (Å) and Angles (deg) in the Complexes Pt((*R*,*R*)-Me-Duphos)(Ph)(X) (X = Cl (1), Br (7), OH (6))

	7	**1**[9]	**6**[b]
Pt−C	2.065(4)	2.074(3)	2.054(10)
Pt-P2	2.2028(11)	2.2012(7)	2.195(2)
Pt−P1	2.2755(11)	2.2774(7)	2.289(3)
Pt−X	2.4900(5)	2.3721(7)	2.055(6)
C−Pt−P2	93.51(12)	93.67(8)	93.3(3)
C−Pt−P1	171.26(13)	170.79(9)	177.4(3)
P2−Pt−P1	87.00(4)	86.99(3)	86.44(9)
C−Pt−X	89.30(11)	89.47(8)	87.8(3)
P2−Pt−X	175.14(3)	175.22(2)	177.4(2)
P1−Pt−X	90.84(3)	90.50(3)	92.6(2)

[a] Labeling: P1 is trans to Ph, P2 is trans to X. [b] Two independent molecules in the unit cell; average value. Note that the P atom numbering in Figure 1 is reversed from the convention in this table.

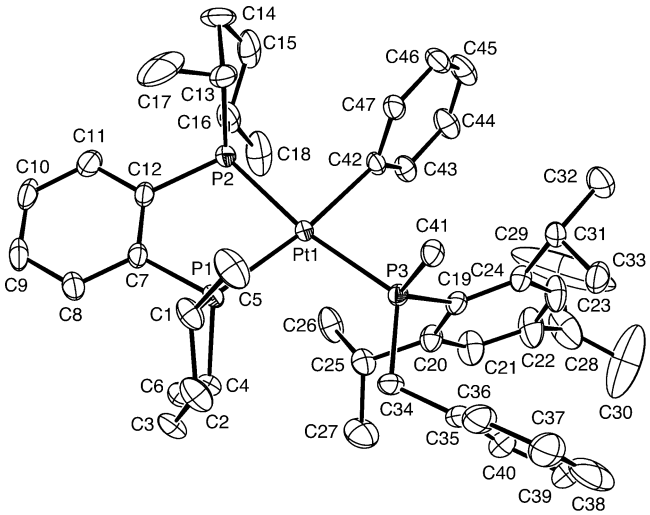

Figure 7. ORTEP diagram of [Pt((*R*,*R*)-Me-Duphos)(Ph)(PMeIs-(CH_2Ph))][BF_4] (**8-BF_4**). The BF_4 anion and disorder involving C atoms 14, 15, 17, 28, 29, 30, and 38 are omitted.

in phosphido complex **4** (2.3761(13) Å) shortened to 2.3126(13) Å on protonation (**12**) and to 2.3338(8) Å on alkylation (**8-BF_4**), perhaps because quaternization eliminated repulsive Pt−P π-interactions.[17] The Pt−Ph bonds became slightly longer on quaternization, changing from 2.070(5) Å in **4** to 2.082(4) Å in **12** and 2.093(3) Å in **8-BF_4**; the shorter Pt−P3 bond might result in greater steric repulsion.

Table 5. Selected Bond Lengths (Å) and Angles (deg) for the Complexes Pt((*R*,*R*)-Me-Duphos)(Ph)(PMeIs) (4), [Pt((*R*,*R*)-Me-Duphos)(Ph)(PHMe(Is))][BF_4]·CH_2Cl_2 (12**·CH_2Cl_2), and [Pt((*R*,*R*)-Me-Duphos)(Ph)(PMeIs(CH_2Ph))][BF_4] (**8-BF_4**)**

	4	**12**·CH_2Cl_2	**8-BF_4**
Pt−P1	2.2849(14)	2.2772(13)	2.2853(9)
Pt−P2	2.3028(13)	2.3096(11)	2.3085(7)
Pt−P3	2.3761(13)	2.3126(13)	2.3338(8)
Pt−X	2.070(5)	2.082(4)	2.093(3)
P1−Pt−P2	85.66(5)	85.52(4)	84.93(3)
P1−Pt−P3	171.47(5)	177.11(4)	171.14(3)
P1−Pt−Ph	89.83(14)	90.21(13)	88.47(9)
P2−Pt−P3	97.37(5)	96.82(4)	103.09(3)
P2−Pt−Ph	173.81(15)	172.02(16)	172.94(9)
P3−Pt−Ph	86.51(14)	87.26(13)	83.35(8)
P3 angles	98.8(2)	103.9(13)	115.60(14)
	109.95(15)	120.38(15)	99.07(15)
	111.89(19)	118.19(19)	102.62(14)
			103.65(11)
			113.59(10)
			122.04(10)[b]
∑ P3 angles	320.6(2)	342.47(19)	*b*

[a] Labeling of the phosphorus atoms: P3 = phosphido in **4**, secondary phosphine in **12**·CH_2Cl_2, tertiary phosphine in **8-BF_4**; P1 = Duphos trans to P3; P2 = Duphos cis to P3. Note that the labeling shown in the ORTEP diagram of the complex **8-BF_4** is slightly different. Data for complexes **4** and **12**·CH_2Cl_2 are taken from ref 11. [b] The complex **8-BF_4** is unique in that bond angles involving all four P substituents could be measured (for the other complexes only three were available). The average angle at P3 was 109.43(15)°.

Table 6. Selected ^{31}P NMR Data (in Hz) and Bond Lengths (Å) for the Terminal and Alkylated/Protonated Phosphido Group in the Complexes 4, 8-BF_4, and 12·CH_2Cl_2[a]

complex	J_{Pt-P} (trans to PR_2)	Pt−P1 (Å)
Pt((*R*,*R*)-Me-Duphos)(Ph)(PMeIs) (**4**)	1621	2.2849(14)
[Pt((*R*,*R*)-Me-Duphos)(Ph)(PMeIs-(CH_2Ph))][BF_4] (**8-BF_4**)	2443, 2459[b]	2.2853(9)
[Pt((*R*,*R*)-Me-Duphos)(Ph)(PHMe(Is))]-[BF_4] (**12**)	2623, 2618[b]	2.2772(13)

[a] Labeling of the phosphorus atoms is as in Table 5: P3 = phosphido in **4**, secondary phosphine in **12**·CH_2Cl_2, tertiary phosphine in **8-BF_4**; P1 = Duphos trans to P3; P2 = Duphos cis to P3. Note that the labeling shown in the ORTEP diagram of complex **8-BF_4** is slightly different. Solvent: CD_2Cl_2 for cations **8** and **12**, C_6D_6 (room temperature) for **4**. Data for **4** and **8** is from ref 11. [b] Data are given for the two diastereomers of **8-BF_4** and **12**.

From the Pt−P1 (trans to P3) bond lengths, which are the same for **4** and **8-BF_4** but a bit shorter for **12**, the apparent trans influence trend would be PMeIs ≈ PMeIs(CH_2Ph) > PHMe(Is).[15] The ^{31}P NMR data (Table 6) showed that J_{Pt-P} for the phosphine trans to the phosphido group increased upon alkylation/protonation, suggesting a PMeIs > PMeIs(CH_2Ph) > PHMe(Is) trans influence series for these ligands.[11]

2. Mechanism and Origin of Enantioselectivity. We investigated the mechanisms of the stoichiometric reactions which interconvert these potential intermediates to learn more about the overall mechanism of catalysis.

(a) Formation of Phosphido Complex 4. We reported previously that treatment of the palladium iodo complex Pd((*R*,*R*)-Me-Duphos)(Ph)(I) (**1-Pd-I**) with PHMe(Is)/$NaOSiMe_3$ led to **4-Pd** via deprotonation of the intermediate cationic secondary phosphine complex [Pd((*R*,*R*)-Me-Duphos)(Ph)(PHMe(Is))][I];[16] no reaction between $NaOSiMe_3$ and PHMe(Is),

(17) (a) Caulton, K. G. *New J. Chem.* **1994**, *18*, 25−41. (b) Holland, P. L.; Andersen, R. A.; Bergman, R. G. *Comments Inorg. Chem.* **1999**, *21*, 115−129.

Scheme 5. Potential Mechanisms for Formation of Phosphido Complexes 4 and 4-Pd[a]

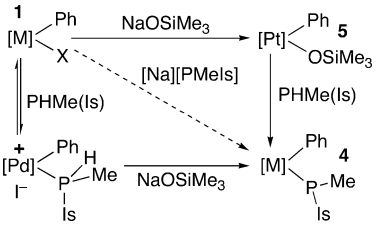

[a] [M] = M((*R*,*R*)-Me-Duphos), M = Pd, Pt.

Scheme 6[a]

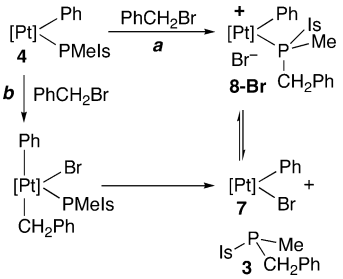

[a] [Pt] = Pt((*R*,*R*)-Me-Duphos).[19b]

Scheme 7[a]

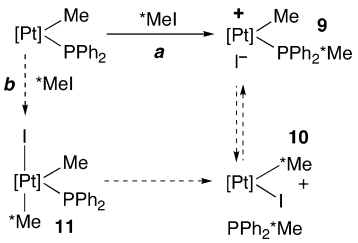

[a] [Pt] = Pt(dppe).[19b]

Scheme 8[a]

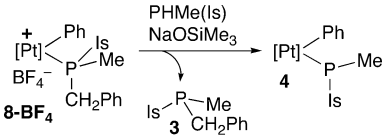

[a] [Pt] = Pt((*R*,*R*)-Me-Duphos).

or between $NaOSiMe_3$ and **1-Pd-I** was observed by NMR spectroscopy (Scheme 5).[4b] In contrast, the Pt chloride **1** did not appear to react with PHMe(Is). Instead, treatment of **1** with PHMe(Is) and $NaOSiMe_3$ gave **4**; this reaction seemed to proceed via formation of the silanolate **5**, followed by proton transfer from the secondary phosphine to yield **4** (Schemes 3 and 5). The latter step presumably occurred by coordination of phosphine **2** to Pt in **5**, which would make the P−H proton more acidic; a four-center transition state for Pt−P and O−H bond formation is plausible, or the ion pair [Pt((*R*,*R*)-Me-Duphos)(Ph)(PHMe(Is))][$OSiMe_3$], formed via displacement of the silanolate ion by **2**, may be involved.[11,18] Since both the metal and the leaving group were changed, we cannot tell which factor controlled the difference in the mechanism of M−P bond formation.

(18) For formation of Pt−phosphido complexes by treatment of a Pt−methoxide complex with primary or secondary phosphines, see: (a) Wicht, D. K.; Paisner, S. N.; Lew, B. M.; Glueck, D. S.; Yap, G. P. A.; Liable-Sands, L. M.; Rheingold, A. L.; Haar, C. M.; Nolan, S. P. *Organometallics* **1998**, *17*, 652−660. (b) Kourkine, I. V.; Sargent, M. D.; Glueck, D. S. *Organometallics* **1998**, *17*, 125−127.

Scheme 9. Possible Mechanisms for Formation of 4 from 8-Br[a]

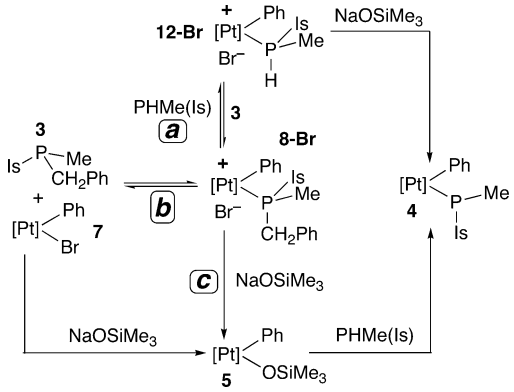

[a] [Pt] = Pt((*R*,*R*)-Me-Duphos).

Scheme 10[a]

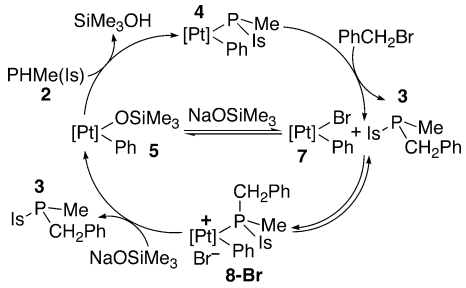

[a] [Pt] = Pt((*R*,*R*)-Me-Duphos).

Scheme 11[a]

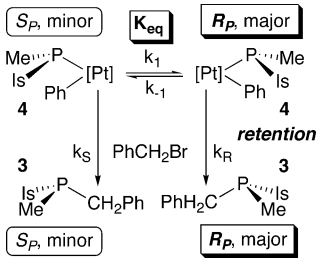

[a] [Pt] = Pt((*R*,*R*)-Me-Duphos).

(b) Alkylation of Phosphido Complex 4. We hypothesized, as in Scheme 1, that P−C bond formation in **4** occurred by direct S_N2 attack of the Pt−phosphido group on benzyl bromide to yield the cation **8-Br** (path a, Scheme 6), followed (in toluene) by displacement of the coordinated phosphine **3** by the bromide counterion. Alternatively, oxidative addition of benzyl bromide to **4** (path b, Scheme 6) might yield a Pt(IV) intermediate, from which selective P−C reductive elimination would give the products **7** and **3**. Although oxidative addition of benzyl bromide to the Pt(II) phosphine complex $Pt(PMe_2Ph)_2Me_2$ is known,[19] P−C reductive elimination from Pt(IV) does not appear to have been reported.[20]

To examine these possibilities in a model system, we treated Pt(dppe)(Me)(PPh_2) with ^{13}C-labeled methyl iodide (*MeI;

(19) (a) Brown, M. P.; Puddephatt, R. J.; Upton, C. E. E.; Lavington, S. W. *J. Chem. Soc., Dalton Trans.* **1974**, 1613−1618. (b) The stereochemistry of the proposed Pt(IV) complexes in Schemes 6 and 7 was drawn arbitrarily by analogy to refs 19a and 22; for more information on the stereochemistry of related complexes, see also: Brown, M. P.; Puddephatt, R. J.; Upton, C. E. E. *J. Chem. Soc., Dalton Trans.* **1974**, 2457−2465. Goldberg, K. I.; Yan, J.; Breitung, E. M. *J. Am. Chem. Soc.* **1995**, *117*, 6889−6896.

(20) For studies of C−O reductive elimination from analogous Pt(IV) complexes, see: Williams, B. S.; Goldberg, K. I. *J. Am. Chem. Soc.* **2001**, *123*, 2576−2587.

Chart 2. ^{1}H and ^{13}C (Boldface Italics) NMR Assignments for the Major Diastereomer of 4 (THF-d_8, −60 °C)

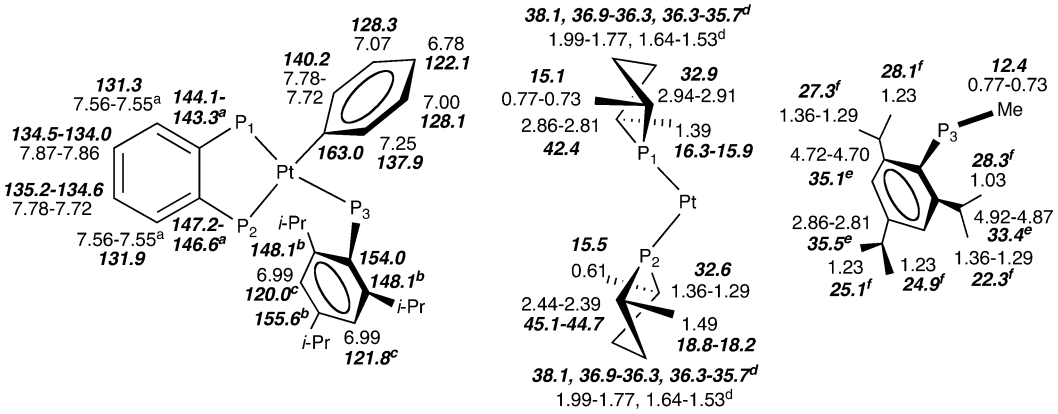

[a] Which Duphos quaternary C atom is adjacent to P_1 (or P_2) could not be determined; similarly, the *o*-Duphos Ar CH signals overlapped. [b] Only two of the three expected ^{13}C NMR signals for the Is *o*- and *p*-quaternary C atoms were observed; we cannot tell the difference between the ortho and para resonances. [c] We cannot tell which Is *m*-C is on which side of the ring because of the coincident ^{1}H NMR shifts of H30 and H35. [d] We could not differentiate the CH_2 groups in the phospholane or unambiguously assign their ^{13}C signals. [e] The assignment of the *o*-CH (*i*-Pr) ^{1}H NMR peaks shown is based on their similar chemical shifts and NOE data. [f] Because of ^{1}H NMR peak overlap of the Me (*i*-Pr) signals, definitive assignment of the corresponding ^{13}C NMR signals was not possible. The assignments shown are consistent with correlations between the *i*-Pr CH and Me signals, but unambiguous assignment of individual peaks to ortho or para positions was not possible.

Scheme 7).[18,21] S_N2 alkylation of the phosphido group (path a) would yield the cation [Pt(dppe)(Me)(PPh_2*Me)][I] (**9**); by analogy to the chemistry of Schemes 4 and 6, it might be in equilibrium with neutral Pt(dppe)(Me)(I) (**10**) and PPh_2*Me, with the carbon label only in the P−*Me group. After oxidative addition of *MeI (path b), however, reductive elimination from the Pt(IV) complex Pt(dppe)(Me)(*Me)(PPh_2)(I) (**11**) would yield **10** and PPh_2Me, with the labeled methyl group scrambled between Pt and P sites. The known reaction of MeI with Pt(dppe)Me_2, which gave the stable Pt(IV) complex Pt(dppe)-Me_3I, suggests that this pathway is plausible.[22]

The experiment of Scheme 7 provided unambiguous evidence for the S_N2 mechanism. Treatment of Pt(dppe)(Me)(PPh_2) with *MeI in toluene-d_8 caused immediate precipitation of cation **9**, which was identified by ^{31}P, ^{13}C, and ^{1}H NMR spectroscopy and by comparison to the reported ^{31}P NMR spectrum of the PF_6 salt;[23] the ^{13}C label was found exclusively in the P site. By analogy, we assume that alkylation of phosphido complex **4** also proceeded by a nucleophilic pathway.

(c) Product Formation and Catalyst Regeneration. Cation **8-Br** was the major Pt complex observed by ^{31}P NMR spectroscopy during catalysis,[24] suggesting that the rate-determining step involved substitution of the coordinated tertiary phosphine **3** with the phosphido ligand. Stoichiometric treatment of **8-BF_4** with PHMe(Is) and $NaOSiMe_3$ gave **3** and regenerated the phosphido complex **4** (Scheme 8).

We considered three possible mechanisms for this step under catalytic conditions (Scheme 9). (a) The simplest would involve ligand substitution, in which PHMe(Is) displaced the bulkier tertiary phosphine to yield [Pt((*R*,*R*)-Me-Duphos)(Ph)(PHMe-(Is))][Br] (**12-Br**). Independently prepared[11] **12-BF_4** reacted quickly with $NaOSiMe_3$ to give **4**; thus, **12-Br** would be a competent intermediate.

However, the proposed ligand substitution via reaction of **8-BF_4** with PHMe(Is) was very slow. This might be due to an unfavorable equilibrium, in which **8-Br** was favored over **12-Br**, although this seems unlikely on steric grounds. This possibility was tested by treating **12-BF_4** with PMeIs(CH_2Ph), but no reaction occurred. We cannot rule out a slowly established equilibrium between cations **8-Br** and **12-Br**, leading to product **4**, but the two other pathways in Scheme 9 appear to be more likely.

(b) From Scheme 4, the cation **8-Br** was in equilibrium with phosphine **3** and bromide **7**. Stoichiometric treatment of **7** with $NaOSiMe_3$/PHMe(Is) yielded the phosphido complex **4** via silanolate **5** (Scheme 9). Catalytic turnover might then plausibly occur by a combination of these two processes. The position of the **8-Br**/**3** + **7** equilibrium during catalysis would depend on the concentration of the bromide anion and that of the tertiary phosphine **3**. NaBr precipitated during the reaction while more phosphine **3** formed, which should favor **8-Br**. Further, the reduced concentration of $NaOSiMe_3$ and PHMe(Is) as the reaction proceeds should slow down the formation of **4** from **7**, reducing the rate of catalyst turnover by this pathway.

(c) In the third possible pathway, the cation **8-Br** reacted with $NaOSiMe_3$ to yield silanolate **5**, which then deprotonated PHMe-(Is), regenerating the Pt−phosphido complex **4**. These reactions were observed directly with **8-BF_4**. On treatment with $NaOSiMe_3$ it was slowly partially converted to **5** in an apparent equilibrium. Silanolate complex **5** then reacted quickly with secondary phosphine **2** to yield phosphido complex **4**.

From these observations of the stoichiometric steps in catalysis, pathways (b) and (c) are most likely responsible for catalytic turnover. The proposed mechanism is summarized in Scheme 10.

Origin of Enantioselectivity. As in Scheme 1, we hypothesized that P inversion in the phosphido intermediate **4** was much faster than alkylation. Under these Curtin−Hammett conditions, is the major product enantiomer formed from the major or the minor Pt−phosphido diastereomer?[25,26] P-alkylation at three-coordinate organophosphorus centers as well as in

(21) Scriban, C.; Wicht, D. K.; Glueck, D. S.; Zakharov, L. N.; Golen, J. A.; Rheingold, A. L. *Organometallics* **2006**, *25*, 3370−3378.

(22) Appleton, T. G.; Bennett, M. A.; Tomkins, I. B. *J. Chem. Soc., Dalton Trans.* **1976**, 439−446.

(23) Goel, A. B.; Goel, S. *Inorg. Chim. Acta* **1982**, *59*, 237−240.

(24) Speciation appeared to depend on concentration and percent conversion during catalysis. In addition to **8-Br**, a small amount of phosphido complex **4** was also observed later in the reaction.

(25) Product racemization via pyramidal inversion should be slow under these conditions (Mislow, K. *Trans. N. Y. Acad. Sci.* **1973**, *35*, 227−242).

(26) (a) Halpern, J. *Science* **1982**, *217*, 401−407. (b) Landis, C. R.; Halpern, J. *J. Am. Chem. Soc.* **1987**, *109*, 1746−1754. (c) Schmidt, T.; Baumann, W.; Drexler, H.-J.; Arrieta, A.; Heller, D.; Buschmann, H. *Organometallics* **2005**, *24*, 3842−3848.

metal−phosphido complexes proceeds with retention of configuration;[27,5c] thus, alkylation of (R_P)-**4** should yield (R_P)-**3** (S_P when it remains complexed to Pt, in the cation **8-BF$_4$**). This matched the experimental observations.[28]

Therefore, the major product ((R_P)-**3**) appears to be formed from the major intermediate ((R_P)-**4**). In contrast to the classic major product from minor intermediate result in asymmetric hydrogenation,[26] these results suggest that enantioselectivity was determined mainly by the thermodynamic preference for one of the rapidly interconverting diastereomers of **4**, although their relative rates of alkylation were also important (Curtin−Hammett kinetics; Scheme 11).

Conclusions

We have presented evidence for the mechanism (Scheme 10) of Pt-catalyzed asymmetric alkylation of a secondary phosphine. Consistent with the hypothesis of Scheme 1, the phosphido complex **4** existed as a mixture of diastereomers, which interconverted via rapid P inversion. Nucleophilic attack on benzyl bromide yielded the product phosphine **3**, which remained coordinated to Pt in the major resting state **8**; thus, as expected, product inhibition slowed catalytic turnover. The two possible routes we identified for turnover (Scheme 9) suggest ways to address this problem in this system and related catalyses. First, a smaller base such as methoxide might favor nucleophilic displacement of the tertiary phosphine (so might a less bulky phosphine, although that might reduce the enantioselectivity). The potential bromide route via **7** suggests that having more bromide available (with a polar solvent or added bromide) might also increase the rate.

Since the major diastereomer of phosphido intermediate **4** appeared to yield the major enantiomer of the product phosphine **3**, catalytic enantioselectivity (Scheme 11) resulted mainly from a thermodynamic preference for one of the diastereomers of **4**. Tuning sterics and electronics of the secondary phosphine substrate and the catalyst might then provide a way to maximize K_{eq} for rational control of enantioselection. However, Scheme 11 and the experimental observation that product ee in the alkylation of PHMe(Is) (**2**) depended on the benzyl bromide substrate[1] emphasize that the rate constants k_S and k_R were also important in enantioselection.

Experimental Section

Unless otherwise noted, all reactions and manipulations were performed in dry glassware under a nitrogen atmosphere at 20 °C in a drybox or using standard Schlenk techniques. Petroleum ether (bp 38−53 °C), ether, THF, toluene, and CH_2Cl_2 were dried using columns of activated alumina.[29] NMR spectra were recorded using Varian 300 and 500 MHz spectrometers. ^{1}H and ^{13}C NMR chemical shifts are reported vs Me_4Si and were determined by reference to the residual ^{1}H and ^{13}C solvent peaks. ^{31}P NMR chemical shifts are reported vs H_3PO_4 (85%) used as an external reference. Coupling constants are reported in Hz as absolute values. Unless indicated, peaks in NMR spectra are singlets. Elemental analyses were provided by Schwarzkopf Microanalytical Laboratory or Quantitative Technologies Inc. Mass spectra were recorded at the University of Illinois Urbana−Champaign.

Reagents were from commercial suppliers, except for these compounds, which were made by the literature procedures: Pt((*R*,*R*)-Me-Duphos)(Ph)(Cl),[9] PMeIs(CH_2Ph),[1] PHMe(Is),[8] Pt((*R*,*R*)-Me-Duphos)(Ph)(PMeIs) and [Pt((*R*,*R*)-Me-Duphos)(Ph)(PHMeIs)][BF_4],[1,11] and Pt(dppe)(Me)(PPh_2).[21]

Generation of Pt((*R*,*R*)-Me-Duphos)(Ph)(OSiMe$_3$) (5). To a stirred slurry of Pt((*R*,*R*)-Me-Duphos)(Ph)(Cl) (**1**; 123 mg, 0.2 mmol) in toluene (0.2 mL) was added a slurry of $NaOSiMe_3$ (22 mg, 0.2 mmol) in 0.3 mL of toluene. The slurry immediately dissolved; the solution was transferred into an NMR tube and monitored by ^{31}P NMR spectroscopy. After 3 days the mixture consisted of Pt((*R*,*R*)-Me-Duphos)(Ph)(OSiMe$_3$) (**5**; 67%), Pt((*R*,*R*)-Me-Duphos)(Ph)(OH) (**6**; 15%), and unreacted Pt((*R*,*R*)-Me-Duphos)(Ph)(Cl) (**1**; 18%). The reaction mixture was added to $NaOSiMe_3$ (7 mg, 0.06 mmol), and according to the ^{31}P NMR spectrum the only species present were Pt((*R*,*R*)-Me-Duphos)(Ph)(OSiMe$_3$) (**5**; major) and Pt((*R*,*R*)-Me-Duphos)(Ph)(OH) (**6**). The reaction mixture was filtered through Celite, and the solvent was removed under vacuum. The ^{31}P NMR spectrum (CD_2Cl_2) of the solution indicated a mixture of Pt((*R*,*R*)-Me-Duphos)(Ph)(OSiMe$_3$) (86%) and Pt((*R*,*R*)-Me-Duphos)(Ph)(OH) (14%). The ^{1}H NMR spectrum (CD_2Cl_2) also showed some impurities; therefore, the solvent was removed under reduced pressure and the white residue was washed with toluene (2 portions of 0.2 mL) and dried under vacuum, yielding white crystals. The parent ion was not observed by ESMS: *m*/*z* 578.1 (Pt((*R*,*R*)-Me-Duphos)(Ph)$^+$), 619.2, 651.2 (Pt((*R*,*R*)-Me-Duphos)(Ph)(SiMe$_3$)$^+$).

Pt((*R*,*R*)-Me-Duphos)(Ph)(OSiMe$_3$) (5; 90% of the Mixture). ^{31}P{^{1}H} NMR (C_6D_6): δ 67.1 (d, J = 4, J_{Pt-P} = 1702), 46.6 (d, J = 4, J_{Pt-P} = 3619). The following ^{1}H NMR (C_6D_6) spectrum is reported as a mixture of **5** (90%) and hydroxide **6** (10%) unless otherwise indicated. ^{1}H NMR (C_6D_6): δ 8.03−7.94 (m, 2H, Ar), 7.37−7.31 (m, 2H, Ar), 7.22−6.94 (m, 5H, Ar), 3.44−3.37 (m, 1H, **6**), 3.35−3.26 (m, 1H, **5**), 3.16−3.07 (m, 1H), 2.40−2.25 (m, 1H), 2.21−1.86 (m, 5H), 1.68 (dd, J = 19, 7, 3H, Me, **6**), 1.61 (dd, J = 18, 7, 3H, Me, **5**), 1.56−1.34 (m, 2H), 1.24 (dd, J = 18, 8, 3H, Me), 1.06−0.87 (m, 2H), 0.72 (dd, J = 15, 8, 3H, Me), 0.65 (dd, J = 16, 7, 3H, Me), 0.33 (9H). ^{13}C{^{1}H} NMR (C_6D_6): δ 164.4 (dd, J = 126, 8, quat, Pt−Ph), 147.0 (dd, J = 47, 38, quat Ar), 143.1 (dd, J = 35, 24, quat Ar), 139.7 (broad, Ph), 133.2 (d, J = 12, Ar), 132.7 (dd, J = 15, 3, Ar), 130.8−130.6 (m, Ar), 128.0 (d, J = 7), 126.0, 123.9 (Ar), 40.51 (d, J = 26), 40.48 (d, J = 39), 37.5, 36.9 (d, J = 4), 36.7, 35.5 (d, J = 6), 33.70 (d, J = 38), 33.69 (d, J = 25), 17.5 (d, J = 10, Me), 16.8 (d, J = 6, Me), 14.44 (d, J = 5, Me), 14.43 (d, J = 5, Me), 6.0 (OSiMe$_3$).

Pt((*R*,*R*)-Me-Duphos)(Ph)(OH) (6). Method I. To a stirred slurry of Pt((*R*,*R*)-Me-Duphos)(Ph)(Cl) (**1**; 61.4 mg, 0.1 mmol) in MeOH (10 mL) was added NaOH (90 mg, 2.3 mmol). After 10 min the solvent was removed under reduced pressure and toluene (10 mL) was added to the white residue. The resulting white slurry was filtered through Celite, and the filtrate was concentrated under vacuum. The ^{31}P NMR spectrum of the filtrate indicated a mixture of **6** (∼35%) and Pt((*R*,*R*)-Me-Duphos)(Ph)(OMe) (∼65%, see the Supporting Information). The solvent was removed under vacuum, and the white powder was redissolved in THF. Water (50 μL, 2.8 mmol) was added via a microliter syringe. After 10 min the solvent was removed under vacuum and toluene (5 mL) was added to the white powder. The ^{31}P NMR spectrum of the solution indicated only **6**. The toluene was removed under vacuum, yielding 39 mg (66%) of white crystals.

Method II. To a stirred slurry of **1** (123 mg, 0.2 mmol) in THF (10 mL) was added H_2O (0.5 mL) and NaOH (80 mg, 2.0 mmol). After 1 h the solvent was removed under reduced pressure and toluene (10 mL) was added to the white residue. The resulting white slurry was filtered through Celite, and the filtrate was concentrated under vacuum. The ^{31}P NMR spectrum of the filtrate indicated a mixture of **6** (∼90%) and unreacted **1** (∼10%). THF (10 mL) was

(27) Quin, L. D. *A Guide to Organophosphorus Chemistry*, Wiley-Interscience: New York, 2000; p 301.

(28) Note that the R_P product was also favored in the alkylation of PHPh(Cy) (Cy = cyclohexyl) to give PPh(Cy)(CH_2Ph) using the same catalyst precursor (**1**).[1]

(29) Pangborn, A. B.; Giardello, M. A.; Grubbs, R. H.; Rosen, R. K.; Timmers, F. J. *Organometallics* **1996**, *15*, 1518−1520.

added to the white powder, followed by H_2O (0.5 mL) and NaOH (80 mg, 2.0 mmol). After 12 h, the solvent was removed under reduced pressure and toluene (10 mL) was added to the white residue. The resulting white slurry was filtered through Celite, and the filtrate was concentrated under vacuum. The ^{31}P NMR spectrum of the filtrate indicated a mixture of **6** (∼95%) and unreacted **1** (∼5%). The solvent was removed under vacuum, yielding 96 mg (81%) of white powder.

Anal. Calcd for $C_{24}H_{34}OP_2Pt$: C, 48.40; H, 5.75. Calcd for $C_{24}H_{34}OP_2Pt\cdot0.05C_{24}H_{33}ClP_2Pt$: C, 48.33; H, 5.74. Found: C, 48.87; H, 5.76. The parent ion was not observed by ESMS: *m*/*z* 578.2 (Pt((*R*,*R*)-Me-Duphos)(Ph)$^+$), 619.2, 791.4, 1182.5. $^{31}P\{^1H\}$ NMR (C_6D_6): δ 67.6 (d, $J = 5$, $J_{Pt-P} = 1803$), 48.7 (d, $J = 5$, $J_{Pt-P} = 3218$). ^1H NMR (C_6D_6): δ 7.99 (t, $J = 13$, $J_{Pt-P} = 43$, 2H, Ar), 7.35−7.32 (m, 2H, Ar), 7.22−7.19 (m, 1H, Ar), 7.14−7.08 (m, 2H, Ar), 7.01−6.97 (m, 2H, Ar), 3.49−3.43 (m, 1H), 3.16−3.07 (m, 1H), 2.40−2.32 (m, 1H), 2.19−2.10 (m, 2H), 2.03−1.91 (m, 2H), 1.82 (broad, 1H), 1.68 (dd, $J = 19$, 7, 3H, Me), 1.63−1.32 (m, 2H), 1.31−1.21 (m, 1H), 1.21 (dd, $J = 18$, 7, 3H, Me), 1.11−0.92 (m, 2H), 0.75 (dd, $J = 15$, 7, 3H, Me), 0.68 (dd, $J = 16$, 8, 3H, Me). $^{13}C\{^1H\}$ NMR (C_6D_6): δ 166.8 (dd, $J = 121$, 7, quat, Pt−Ph), 147.1 (dd, $J = 45$, 38, quat Ar), 143.5 (dd, $J = 35$, 25, quat Ar), 138.5 ($J_{Pt-C} = 22$, Ph), 133.3 (d, $J = 13$, Ar), 132.8 (dd, $J = 14$, 3, Ar), 130.8−130.6 (m, Ar), 124.2 (Ar), 40.2 (d, $J = 27$), 39.8 (d, $J = 36$), 37.5, 36.71, 36.67 (d, $J = 4$), 35.6 (d, $J = 6$), 34.3 (d, $J = 25$), 34.0 (d, $J = 36$), 18.1 (d, $J = 11$, Me), 17.3 (d, $J = 6$, Me), 14.49 (d, $J = 4$, Me), 14.47 (d, $J = 3$, Me). Note: hydroxide complex **6** took up CO_2 from the air to yield (Pt((*R*,*R*)-Me-Duphos)(Ph))$_2$(μ-CO_3), which was characterized crystallographically (see the Supporting Information).

Stoichiometric Reaction of Pt((*R*,*R*)-Me-Duphos)(Ph)(Cl) (1) with NaOSiMe$_3$/PHMe(Is). Generation of Pt((*R*,*R*)-Me-Duphos)(Ph)(PMeIs) (4) in Situ. A slurry of $NaOSiMe_3$ (11 mg, 0.1 mmol) in 0.5 mL of toluene was added to **1** (61.4 mg, 0.1 mmol). The resulting colorless solution was transferred into an NMR tube. The components of the mixture, observed by ^{31}P NMR spectroscopy, were chloride **1** and silanolate **5** (3.5:1). A very small amount of hydroxide **6** could also be detected. The solution was added to PHMe(Is) (**2**; 25 mg, 0.1 mmol); the mixture turned yellow immediately. Complex **4** was the major component along with a small amount of **5**, indicating that a substoichiometric amount of secondary phosphine was added. The mixture was added to 6 mg of PHMe(Is) (0.024 mmol); then, **4** was the only Pt species observed, along with a small excess of PHMe(Is).

Reaction of Pt((*R*,*R*)-Me-Duphos)(Ph)(PMeIs) (4) Generated in Situ with 1 Equiv of PhCH$_2$Br Followed by Treatment with NaOSiMe$_3$/PHMe(Is). To the above mixture was added benzyl bromide (17 mg, 12 μL, 0.1 mmol) via a microliter syringe. The mixture became light yellow in less than 30 min. Only Pt((*R*,*R*)-Me-Duphos)(Ph)(Br) (**7**) and PMeIsCH$_2$Ph (**3**) were observed by ^{31}P NMR spectroscopy, but the light yellow color was consistent with the presence of a small amount of the phosphido complex (see below). This reaction mixture was added to $NaOSiMe_3$ (11 mg, 0.1 mmol); it remained yellow. After 1 h, complexes **7** and Pt((*R*,*R*)-Me-Duphos)(Ph)(OSiMe$_3$) (**5**) (12:1) were the major Pt species observed, along with **3**. Small amounts of **4**, cation **8**, and hydroxide **6** could also be detected. The presence of **4** was probably due to addition of a substoichiometric amount of PhCH$_2$Br in the previous step; therefore, after 1 day 2 μL of PhCH$_2$Br (3 mg, 0.017 mmol) was added. The color faded in ∼5 min. Complexes **7**, **5**, and **6** (ratio 12.8:17.1:1), along with a small amount of **8**, and phosphine **3** were observed.

The solution was added to PHMe(Is) (25 mg, 0.1 mmol). The mixture turned yellow immediately. After 5 min ^{31}P NMR monitoring showed the presence of **4**, **7**, and **3**, along with a small amount of **8**. After 15 min some silanolate **5** was also detected. Since no PHMe(Is) was observed, 5 mg of PHMe(Is) (0.02 mmol) was added. After 15 min phosphido complex **4** and phosphine **3** were the major components of the mixture. Unreacted PHMe(Is) was also present. A small amount of cation **8** could also be detected. After 45 min the ratio **3**:**2** was 7.9:1. The mixture was unchanged the next day.

Stoichiometric Reaction of Pt((*R*,*R*)-Me-Duphos)(Ph)(PMeIs) (4) with Benzyl Bromide. Synthesis of Pt((*R*,*R*)-Me-Duphos)(Ph)(Br) (7). A solution of Pt((*R*,*R*)-Me-Duphos)(Ph)(PMeIs) (**4**; 124.2 mg, 0.15 mmol) in toluene (5 mL) was transferred into an NMR tube, which was fitted with a septum. The tube was cooled in a NaCl/ice bath at −5 °C. Benzyl bromide (26 mg, 18 μL, 0.15 mmol) was added via a microliter syringe, and the reaction mixture was kept at −15 °C for 10 h, when the reaction was completed, according to ^{31}P NMR. Complex **7** and PMeIs(CH$_2$Ph) (**3**) were the only components of the mixture observed in toluene. The solvent was removed under vacuum, and 5 mL of petroleum ether was added to the white solid. The solid was allowed to settle, and the liquid was removed with a pipet. The white solid was further washed with three 5 mL portions of petroleum ether, dried under vacuum, and redissolved in CD_2Cl_2. Complex **7** (41%) and PMeIs(CH$_2$Ph) (36%) were observed as the major components of the mixture, along with 23% of **8-Br**, which was independently synthesized as the BF_4 salt (see below). The solvent was removed under vacuum, and 5 mL of a 9:1 mixture of petroleum ether and THF was added to the residue. The resulting white precipitate was washed with five 5 mL portions of 9:1 petroleum ether−THF. The washes were collected, and the tertiary phosphine was isolated by filtration on a silica column (5 cm height, 0.6 cm diameter), using a 9:1 petroleum ether−THF mixture as eluent, followed by solvent removal under vacuum, yielding 38 mg of a colorless oil (75% yield). The white precipitate (**7**) was dried under vacuum and recrystallized from THF/petroleum ether at −10 °C, yielding 80 mg (82%) of white crystals suitable for X-ray crystallography. Similar experiments in which the ee of **3** was measured are described in the Supporting Information.

Anal. Calcd for $BrC_{24}H_{33}P_2Pt$: C, 43.78; H, 5.05. Found: C, 43.85; H, 4.97. $^{31}P\{^1H\}$ NMR (CD_2Cl_2): δ 66.0 (d, $J = 6$, $J_{Pt-P} = 1647$), 56.8 (d, $J = 6$, $J_{Pt-P} = 3960$). ^1H NMR (CD_2Cl_2): δ 7.78−7.73 (m, 1H), 7.66−7.56 (m, 3H), 7.47 (t, $J = 7$, $J_{Pt-H} = 36$, 2H, Ar), 7.10 (td, $J = 8$, 2, 2H), 6.88 (t, $J = 7$, 1H), 3.49−3.40 (m, 1H), 3.32−3.16 (m, 1H), 2.86−2.74 (m, 1H), 2.74−2.53 (m, 1H), 2.44−2.24 (m, 2H), 2.13−1.97 (m, 2H), 1.94−1.82 (m, 1H), 1.82−1.72 (m, 1H), 1.64−1.54 (m, 1H), 1.45 (dd, $J = 19$, 7, 3H, Me), 1.19 (dd, $J = 19$, 7, 3H, Me), 0.94−0.87 (m, 6H, Me), 0.84−0.74 (m, 1H). $^{13}C\{^1H\}$ NMR (CD_2Cl_2): δ 138.3 (Ph), 132.9 (d, $J = 13$, Ar), 132.6 (m, Ar), 131.6−131.4 (m, Ar), 127.7 (d, $J = 7$, Ph), 122.9 (Ph), 41.7 (d, $J = 7$), 41.5, 37.6, 37.0 (d, $J = 3$), 36.5, 35.8 (d, $J = 29$), 35.2 (d, $J = 6$), 33.2 (d, $J = 38$), 17.2 (d, $J = 9$, Me), 16.0 (d, $J = 5$, Me), 14.3 (d, $J = 19$, 2Me). The quaternary aryl carbons were not observed.

Stoichiometric Reaction of Pt((*R*,*R*)-Me-Duphos)(Ph)(PMeIs) (4) with Benzyl Bromide, Followed by Treatment with PHMe(Is)/NaOSiMe$_3$. An orange solution of **4** (33 mg, 0.04 mmol) in toluene (5 mL) was transferred into an NMR tube, which was fitted with a septum. Benzyl bromide (7 mg, 5 μL, 0.04 mmol) was added via a microliter syringe. After 10 min the color bleached and the reaction was almost complete, according to ^{31}P NMR spectroscopy. Bromide **7** and PMeIs(CH$_2$Ph) (**3**) were observed, plus a trace of **4**.

The reaction mixture was added to 1 equiv of PHMe(Is) (10 mg, 0.04 mmol). Initially, the solution turned yellow, but after ∼30 s the color bleached again. The ^{31}P NMR spectrum showed **7**, **3**, and **2** (the ratio of tertiary to secondary phosphine was ∼1:1). The mixture was added to 1 equiv of $NaOSiMe_3$ (5 mg, 0.04 mmol). The mixture turned orange, and a small amount of precipitate was observed. This mixture contained **4** (∼60% of the Pt species) and **3**, along with **7** and a small amount of **8-Br** (∼10% of the Pt

species). This is consistent with the presence of a slight excess of benzyl bromide, which was shown to react with **4** under similar conditions to yield **7** and cation **8**.

Generation of Pt((*R*,*R*)-Me-Duphos)(Ph)(PMeIs) (4) and Its Reactions with Benzyl Bromide and PHMe(Is)/NaOSiMe$_3$. A solution of PHMe(Is) (10 mg, 0.04 mmol) in 0.2 mL of toluene was added to a suspension of $NaOSiMe_3$ (5 mg, 0.04 mmol) in 0.2 mL of toluene. The resulting colorless solution was added to a suspension of Pt((*R*,*R*)-Me-Duphos)(Ph)(Cl) (**1**; 25 mg, 0.04 mmol) in 0.1 mL of toluene. The mixture turned yellow immediately, indicating the formation of **4**. The mixture was transferred into an NMR tube, which was fitted with a septum. Benzyl bromide (7 mg, 5 μL, 0.04 mmol) was added via a microliter syringe. The color bleached in less than 5 min, and the major components of the mixture were **7** and **3**, plus small amounts of **8-Br** and **4**, presumably because a substoichiometric amount of benzyl bromide was added.

$NaOSiMe_3$ (5 mg, 0.04 mmol) and PHMe(Is) (10 mg, 0.04 mmol) were added. The mixture turned yellow immediately, and ^{31}P NMR spectroscopy showed that **4** and **3** were the main components of the mixture, along with a small amount of **8-Br** and **2** (the ratio of **3** to **2** was 1.9:1). Evidently a slight excess of the secondary phosphine was added.

[**Pt((*R*,*R*)-Me-Duphos)(Ph)(NCMe)][BF$_4$].** To a stirred solution of Pt((*R*,*R*)-Me-Duphos)(Ph)(Cl) (**1**; 92.1 mg, 0.15 mmol) in MeCN (15 mL) was added $AgBF_4$ (29.2 mg, 0.15 mmol). An off-white precipitate, which turned black over time, formed immediately. The mixture was filtered through Celite, yielding a pale brown solution. The solvent was removed under vacuum, and petroleum ether (5 mL) was added to the pale brown residue. The solvent was removed with a pipet, and the pale brown precipitate was dried under vacuum, yielding 105 mg (99%) of off-brown powder. The solid was redissolved in CH_2Cl_2 and filtered through Celite, yielding a colorless solution. The solvent was removed under vacuum, and the white residue was washed with 5 mL of petroleum ether and dried under vacuum, yielding an off-white powder. This complex was not obtained in analytically pure form, presumably because of the presence of trace silver salts (brown color), but it could be used successfully (either as generated, or after isolation) to prepare the cation **8-BF$_4$** by displacement of MeCN with the phosphine PMeIs-(CH_2Ph).

Anal. Calcd for $C_{26}H_{36}NP_2PtBF_4$: C, 44.21; H, 5.14; N, 1.98. Calcd for $C_{26}H_{36}NP_2PtBF_4$·0.05AgCl: C, 43.76; H, 5.09; N, 1.96. Found: C, 43.55; H, 5.08; N, 1.57. HRMS: *m*/*z* calcd for ($C_{26}H_{36}NP_2Pt$)$^+$ (M^+), 618.1950; found, 618.1949. ^{31}P{^{1}H} NMR (CD_2Cl_2): δ 71.4 (d, J = 4, J_{Pt-P} = 1656), 50.5 (d, J = 4, J_{Pt-P} = 4085). ^{1}H NMR (CD_2Cl_2): δ 7.84−7.78 (m, 1H), 7.75−7.68 (m, 3H), 7.50−7.46 (m, J_{Pt-H} = 35, 2H), 7.24−7.20 (m, 2H), 7.04 (t, J = 8, 1H), 3.24−3.12 (m, 1H), 3.02−2.89 (m, 2H), 2.76−2.64 (m, 1H), 2.57−2.42 (m, 2H), 2.44 (3H, NCCH_3), 2.14−2.04 (m, 1H), 2.02−1.89 (m, 1H), 1.88−1.77 (m, 1H), 1.72−1.57 (m, 2H), 1.41 (dd, J = 19, 7, 3H, CH_3), 1.21 (dd, J = 19, 7, 3H, CH_3), 0.98−0.89 (m, 6H, 2CH_3), 0.82−0.70 (m, 1H). ^{13}C{^{1}H} NMR (CD_2Cl_2): δ 155.6 (dd, J = 101, 8, quat), 141.5 (dd, J = 54, 36, quat), 138.5 (dd, J = 42, 21, quat), 137.4 (Ar), 133.6 (d, J = 11, Ar), 133.0 (d, J = 5, Ar), 132.9−132.8 (m, Ar), 128.5 (d, J = 6, J_{Pt-C} = 42, Ar), 124.6 (Ar), 123.9 (d, J = 6, CN), 41.8 (d, J = 42, CH), 40.7 (d, J = 29, CH), 37.1 (overlapping d, J = 28, CH + CH_2), 36.8 (d, J = 5, CH_2), 36.4 (CH_2), 35.0 (d, J = 6, CH_2), 33.7 (d, J = 40, CH), 17.7 (d, J = 8, CH_3), 16.0 (d, J = 3, J_{Pt-C} = 40, CH_3), 14.2 (d, J = 3, CH_3), 14.0 (d, J = 2, CH_3), 3.7 (NCCH_3).

[**Pt((*R*,*R*)-Me-Duphos)(Ph)(PMeIs(CH_2Ph))][BF$_4$] (8-BF$_4$).** To a stirred solution of [Pt((*R*,*R*)-Me-Duphos)(Ph)(NCMe)][BF_4] (66.4 mg, 0.94 mmol) in MeCN (15 mL) was added PMeIs(CH_2Ph) (31 mg, 0.94 mmol, prepared catalytically at −5 °C, 82% ee). The solvent was removed under vacuum, and petroleum ether (5 mL) was added to the white residue. A white precipitate formed. The solvent was removed with a pipet, and the precipitate was dried under vacuum, yielding 90 mg (95%) of white powder. (Note: if a trace of silver salts remained in the nitrile complex precursor (see above), then a small amount of what appears to be the silver−phosphine complex [Ag(PMeIs(CH_2Ph))]$^+$ was also formed (^{31}P-{^{1}H} NMR (CD_2Cl_2): δ −17.4, $J_{^{107/109}Ag-P}$ = 528, 616).) Recrystallization from CH_2Cl_2/Et_2O gave crystals suitable for X-ray crystallography and elemental analyses. Anal. Calcd for $C_{47}H_{66}P_3PtBF_4$: C, 56.12; H, 6.61. Found: C, 55.74; H, 6.70. HRMS: *m*/*z* calcd for $C_{47}H_{66}P_3Pt^+$ (M^+), 917.4004; found, 917.4011.

^{31}P NMR spectroscopy showed a mixture of the two diastereomers **a** and **b** (the ratio of **a** to **b** was ∼10:1). The following NMR spectra are reported for the major diastereomer **a**, unless otherwise indicated. ^{31}P{^{1}H} NMR (CD_2Cl_2, 21 °C): diastereomer **a**, δ 64.7 (broad, J_{Pt-P} = 1705), 58.2 (dd, J = 370, 6, J_{Pt-P} = 2443), 0.1 (d, J = 370, J_{Pt-P} = 2500); diastereomer **b**, δ 58.25 (dd, J = 366, 8, J_{Pt-P} = 2459), 59.2 (broad, J_{Pt-P} ≈ 1730), −5.7 (d, J = 366). ^{1}H NMR (CD_2Cl_2, 21 °C): δ 7.99−7.95 (m, 1H), 7.81−7.75 (m, 1H), 7.75−7.66 (m, 3H), 7.34 (m, J_{Pt-P} = 35, 1H), 7.26 (broad, 1H), 7.18 (t, J = 8, 1H), 7.16−7.11 (m, 1H), 7.07 (t, J = 8, 2H), 6.85 (t, J = 7, 1H), 6.77 (broad, 1H), 6.65 (broad, 1H), 6.45 (1H, Ar), 6.44 (1H, Ar), 4.22 (broad, 1H), 3.94 (broad, 1H, P−CH_2), 3.22 (broad d, J = 12, 1H, P−CH_2), 3.20−3.06 (overlapping m, 2H), 3.00−2.83 (m, 2H), 2.71−2.53 (broad m, 2H), 2.29−2.16 (broad m, 1H), 2.14−1.88 (m, 5H), 1.85−1.74 (m, 2H), 1.55−1.47 (broad m, 9H, CH_3), 1.292 (d, J = 7, 3H, CH_3, Is), 1.288 (d, J = 7, 3H, CH_3, Is), 1.19 (dd, J = 19, 8, 6H, CH_3), 1.28−1.17 (m, 3H, P−CH_3, overlapping the other peaks), 0.80 (dd, J = 16, 7, 3H, CH_3), 0.36 (broad, 3H, CH_3), 0.12 (broad, 3H, CH_3). ^{13}C{^{1}H} NMR (CD_2Cl_2, 21 °C): δ 155.2 (m, quat), 152.7 (m, quat), 151.0−150.7 (m, quat), 141.6−141.3 (m, quat), 138.8−138.4 (m, quat), 134.3−133.9 (m, Ar), 133.6 (d, J = 5, Ar), 133.5 (d, J = 5, Ar), 133.2 (broad, Ar), 133.1−132.8 (m, Ar), 132.6 (broad, Ar), 130.1 (m, Ar), 128.6 (m, Ar), 128.0−127.6 (broad m, Ar), 124.8 (broad, Ar), 123.7 (m, Ar), 123.4 (m, Ar), 44.8−44.1 (m), 42.9−42.3 (m), 41.1−40.6 (m), 39.7 (dd, J = 26, 3), 37.9−37.6 (broad m), 37.1 (broad), 36.1, 35.0−34.8 (m), 34.4 (d, J = 7) overlapping with 34.6−34.0 (broad), 33.0 (dd, J ≈ 35, 5, CH), 29.6 (broad), 27.9 (broad), 25.6, 25.1−24.8 (broad m), 23.9 (d, J = 4) overlapping with 24.1−23.6 (broad m), 18.9−18.6 (m), 15.5−15.1 (m), 14.8 (d, J = 6), 14.6, 13.8−13.2 (m). ^{31}P{^{1}H} NMR (CD_2Cl_2, −20 °C): diastereomer **a**, δ 64.4 (dd, J = 14, 6, J_{Pt-P} = 1695), 57.9 (dd, J = 368, 6, J_{Pt-P} = 2434), 0.9 (dd, J = 368, 14, J_{Pt-P} = 2490); diastereomer **b**, δ 58.6 (dd, J = 17, 7, J_{Pt-P} = 1731), 58.1 (dd, J = 364, 7, J_{Pt-P} = 2448), −5.7 (d, J = 364, J_{Pt-P} = 2563, overlapping the satellite peaks of diastereomer **a**). ^{1}H NMR (CD_2Cl_2, −20 °C): δ 7.96−7.93 (m, 1H), 7.80−7.74 (m, 1H), 7.74−7.63 (m, 3H), 7.39−7.27 (m, 1H), 7.24 (m, 1H), 7.16 (t, J = 8, 1H), 7.14−7.07 (m, 1H), 7.07−6.96 (m, 2H), 6.83 (t, J = 8, 1H), 6.73−6.67 (broad m, 1H), 6.65−6.60 (broad m, 1H), 6.39 (1H, Ar), 6.38 (1H, Ar), 4.24−4.14 (m, 1H), 3.90 (dd, J = 14, 7, 1H, P−CH_2), 3.16 (dm, J = 14, 1H, P−CH_2), 3.18−3.00 (overlapping m, 2H), 3.00−2.75 (m, 2H), 2.70−2.47 (m, 2H), 2.24−2.15 (m, 1H), 2.08−1.82 (m, 5H), 1.81−1.70 (m, 2H), 1.56 (d, J = 7, 3H, CH_3, Is), 1.51 (dd, J = 19, 7, 3H, CH_3), 1.46 (d, J = 6, 3H, CH_3, Is), 1.262 (d, J = 7, 3H, CH_3, Is), 1.255 (d, J = 7, 3H, CH_3, Is), 1.19 (dd, J = 16, 7, 3H, CH_3), 1.17 (dd, J = 19, 7, 3H, CH_3), 1.23−1.09 (m, 3H, P−CH_3, obscured by the other peaks), 0.77 (dd, J = 16, 7, 3H, CH_3), 0.33 (d, J = 7, 3H, CH_3, Is), 0.02 (d, J = 7, 3H, CH_3, Is).

Reaction of 8-BF$_4$ with Excess [NOct$_4$][Br]. A solution of [$NOct_4$][Br] (41 mg, 0.075 mmol, 5 equiv) in 0.3 mL of toluene was added to a slurry of **8-BF$_4$** (15 mg, 0.015 mmol, highly diastereomerically enriched) in toluene (0.2 mL). The mixture became a colorless homogeneous solution immediately. It was transferred into an NMR tube and monitored by ^{31}P NMR spectroscopy. After 30 min, the bromide **7** and PMeIs(CH_2Ph) (**3**) were the only components of the mixture.

Formation of [Pt(dppe)(Me)(PPh_2*Me)][I] from the Reaction of Pt(dppe)(Me)(PPh_2) and ^{13}C-Labeled *MeI. A yellow solution of Pt(dppe)(Me)(PPh_2) (39.7 mg, 0.05 mmol) in toluene-d_8 (0.5 mL) was transferred to an NMR tube, which was fitted with a septum. $^{13}CH_3I$ (3.1 μL, 7.1 mg, 0.05 mmol) was added via a microliter syringe. A white precipitate formed immediately, and the solution turned colorless. ^{31}P NMR spectroscopy (toluene-d_8) did not show any signal, and ^{1}H and ^{13}C NMR spectra showed only signals due to toluene-d_8. The solvent was removed with a pipet, and the white precipitate was washed with toluene (0.5 mL) and dried under vacuum to give 45 mg (97% yield) of white powder, which was characterized by multinuclear NMR spectroscopy.

$^{31}P\{^1H\}$ NMR (CD_2Cl_2): δ 54.1 (ddd, J = 384, 6, J_{P-C} = 3, J_{Pt-P} = 2690), 49.7 (ddd, J = 19, 6, J_{P-C} = 4, J_{Pt-P} = 1776), 8.2 (ddd, J = 384, 19, J_{P-C} = 36, J_{Pt-P} = 2726), consistent with the literature data for the PF_6 salt in CH_2Cl_2/C_6D_6.[23] ^{1}H NMR (CD_2Cl_2): δ 7.70−7.56 (m, 10H, Ar), 7.56−7.51 (m, 2H, Ar), 7.51−7.40 (m, 10H, Ar), 7.36−7.29 (m, 4H, Ar), 7.29−7.21 (m, 4H, Ar), 2.39 (apparent dt, J = 19, 11, 3H, P−*Me), 2.08−1.97 (m, 2H), 1.82−1.71 (m, 2H), 0.48 (apparent q, J = 7, J_{Pt-H} = 59, 3H, Pt−Me). $^{13}C\{^1H\}$ NMR (CD_2Cl_2): δ 133.7 (d, J = 11, J_{Pt-C} = 22, Ar), 133.5 (d, J = 12, J_{Pt-C} = 14, Ar), 132.58 (d, J = 11, J_{Pt-C} = 20, Ar) overlapping with 132.58 (d, J = 2, Ar), 132.3 (d, J = 2, Ar), 131.4 (d, J = 2, Ar), 130.6 (d, J = 55, quat Ar), 129.78 (d, J = 11, Ar), 129.75 (d, J = 10, Ar), 129.1 (d, J = 11, Ar), 128.2 (d, J = 49, quat Ar), 127.1 (d, J = 55, quat Ar), 32.0−31.5 (m, CH_2), 29.3−28.7 (m, CH_2), 13.8 (very intense apparent dt, J = 36, 3, J_{Pt-C} = 29, P-*Me), 1.00 (dm, J = 73, Pt−Me).

^{31}P NMR Monitoring of the Catalytic Reaction of Benzyl Bromide with PHMe(Is). To PHMe(Is) (150 mg, 0.6 mmol) in 0.2 mL of toluene was added $NaOSiMe_3$ (67.3 mg, 0.6 mmol) suspended in 0.2 mL of toluene. The mixture was added to catalyst precursor **1** (18 mg, 0.03 mmol, 5 mol %) in 0.1 mL of toluene. The reaction mixture was transferred to an NMR tube. Benzyl bromide (71 μL, 103 mg, 0.6 mmol) was added via microliter syringe, and the reaction mixture was monitored by ^{31}P NMR spectroscopy. After 5 min, and again after 1.5 h (∼10% conversion), **8-Br** was observed as the resting state of the catalyst. An increasing amount of white precipitate was observed as the reaction progressed. The reaction was complete after 18 h, when ^{31}P NMR monitoring showed the presence of **7** along with several other unidentified species. In a similar experiment on half the scale, the same resting state was also observed later in the reaction (∼30% conversion).

[Pt((*R*,*R*)-Me-Duphos)(Ph)(PMeIs(CH_2Ph))][Br] (8-Br). $^{31}P\{^1H\}$ NMR (toluene): diastereomer **a**, δ 64.5 (J_{Pt-P} = 1692), 58.1 (d, J = 369, J_{Pt-P} = 2498), −0.2 (d, J = 369, J_{Pt-P} = 2507); diastereomer **b**, δ 58.5 (broad), 58.2 (d, J = 369, J_{Pt-P} = 2436), −6.1 (d, J = 369).

Stoichiometric Reaction of Pt((*R*,*R*)-Me-Duphos)(Ph)(Br) (7) with PHMe(Is), PMeIs(CH_2Ph), and $NaOSiMe_3$. A solution of PHMe(Is) (10 mg, 0.04 mmol) in 0.3 mL of toluene was added to a solution of **7** (26.3 mg, 0.04 mmol) in toluene (0.2 mL). The mixture was transferred into an NMR tube and monitored by ^{31}P NMR spectroscopy. No reaction was observed after 1 h. The solution was added to PMeIs(CH_2Ph) (13.6 mg, 0.04 mmol). Monitoring by ^{31}P NMR spectroscopy showed no reaction, even after 1 day. The mixture was then added to $NaOSiMe_3$ (4.5 mg, 0.04 mmol). The solution turned yellow immediately. After 5 min the only Pt species observed by ^{31}P NMR spectroscopy was **4**. The ratio of **2** to **3** was ∼1:2.6, indicating that there was an excess of PHMe(Is).

Stoichiometric Reaction of [Pt((*R*,*R*)-Me-Duphos)(Ph)(PMeIs(CH_2Ph))][BF_4] (8-BF_4) with PHMe(Is)/$NaOSiMe_3$. A solution of PHMe(Is) (5 mg, 0.02 mmol) in 0.3 mL of toluene was added to a slurry of **8-BF_4** (20 mg, 0.02 mmol, highly diastereomerically enriched) in toluene (0.2 mL). The mixture was monitored by ^{31}P NMR spectroscopy; the cation was soluble enough to give weak NMR signals. A very small amount of PMeIs(CH_2Ph) (**3**) was observed after 2 days. The solution, which contained mostly PHMe(Is), was decanted, and the solid was dried under vacuum, yielding ∼8 mg of white powder, which was dissolved in 0.5 mL of CH_2Cl_2. The solution was transferred into an NMR tube; it consisted of unreacted **8-BF_4** and PHMe(Is), according to ^{31}P NMR spectroscopy. No reaction was observed after 4 days. PHMe(Is) (5 mg, 0.02 mmol) was added, and the solvent was removed under vacuum, yielding a viscous colorless residue, to which a slurry of $NaOSiMe_3$ (2 mg, 0.02 mmol) in toluene (0.5 mL) was added. The mixture turned yellow in ∼30 s. After 1 h phosphido **4** was the only Pt species observed, along with **3** and unreacted **2**, indicating that excess PHMe(Is) (**2**) was present.

Stoichiometric Reaction of [Pt((*R*,*R*)-Me-Duphos)(Ph)(PHMe(Is))][BF_4] (12-BF_4) with PMeIs(CH_2Ph). A solution of PMeIs(CH_2Ph) (9 mg, 0.025 mmol) in 0.3 mL of toluene was added to a slurry of **12-BF_4** (23 mg, 0.025 mmol) in toluene (0.2 mL). The mixture was monitored by ^{31}P NMR spectroscopy; the cation was soluble enough to give weak NMR signals. After 45 min the only Pt species observed was **12-BF_4.** A broad peak was also observed for PMeIs(CH_2Ph). The mixture remained unchanged after two weeks.

Stoichiometric Reaction of [Pt((*R*,*R*)-Me-Duphos)(Ph)(PMeIs(CH_2Ph))][BF_4] (8-BF_4) with $NaOSiMe_3$/PHMe(Is). A solution of **8-BF_4** (20 mg, 0.02 mmol, containing ∼1% of P(O)MeIs(CH_2Ph) impurity) in THF (0.2 mL) was added to $NaOSiMe_3$ (2 mg, 0.02 mmol). Formation of PMeIs(CH_2Ph) was observed as early as 30 min by ^{31}P NMR. After 1 day the amount of PMeIs(CH_2Ph) increased, and silanolate **5** and hydroxide **6** were observed, along with unreacted **8-BF_4** (6.8:1:11.4 ratio). The solution was light purple. After 3 days the ratio became 3:1:1.9. The mixture was added to PHMe(Is) (5 mg, 0.02 mmol). The mixture changed to yellow in ∼30 s. After 15 min **4** was already observed, and the ratio of PMeIsCH_2Ph to PHMe(Is) was 1.8:1. After 1 h the ratio became 2:1, and peaks belonging to both **4** and unreacted **8-BF_4** could be observed. A small amount of [Pt((*R*,*R*)-Me-Duphos)(Ph)(PHMe(Is))][BF_4] (**12-BF_4**) could be detected, indicating that a substoichiometric amount of base was added. After 3 h the ratio of **3** to **2** became 2.8:1, and **4** and **12** were the major Pt species. A very small amount of unreacted **8-BF_4** was also observed; it was consumed after 1 day, when the ratio of **3** to **2** was 4:1.

Stoichiometric Reaction of [Pt((*R*,*R*)-Me-Duphos)(Ph)(PMeIs(CH_2Ph))][BF_4] (8-BF_4) with $NaOSiMe_3$ in Toluene. A slurry of highly diastereomerically enriched **8-BF_4** (20 mg, 0.02 mmol) in toluene (0.4 mL) was added to $NaOSiMe_3$ (2 mg, 0.02 mmol) in 0.1 mL of toluene. Formation of PMeIs(CH_2Ph) was observed as early as 45 min. After 2 days solid **8-BF_4** was still present, but the amount of PMeIs(CH_2Ph) increased, and silanolate **5** was observed, along with unreacted **8-BF_4** (ratio 1.9:1).

NMR Structure Determination for Pt((*R*,*R*)-Me-Duphos)(Ph)(PMeIs) (4). As described above, one- and two-dimensional NMR spectroscopy was used to assign the ^{1}H and ^{13}C NMR spectra of the major diastereomer of **4** in THF-d_8 at −60 °C. Chart 2 shows the assignments; note that the assignment of some signals remains ambiguous, as explained in the footnote. A list of these spectroscopic data, including coupling constants, with atom labels as in the solid-state structure (Figure 2) is also included. For details of the NOESY analysis, see the Supporting Information.

^{1}H NMR (−60 °C, THF-d_8; the assignments are as in Table S1 and Chart 2, but see the text and the chart footnote for comments on ambiguous assignments): δ 7.87−7.86 (m, 1H, Ar, Duphos, H15), 7.78−7.72 (m, 2H, overlapping Ar, Duphos H16 and Ph ortho H6), 7.56−7.55 (m, 2H, Ar, Duphos, H14/H17), 7.25 (broad t, J = 7, 1H, Ph ortho, H2), 7.07 (broad t, J = 8, 1H, Ph meta, H5), 7.00 (broad t, J = 8, 1H, Ph meta, H3), 6.99 (2H, Is meta, H30/H35), 6.78 (broad t, J = 8, 1H, Ph para, H4), 4.92−4.87 (m, 1H, CH, Is, H27), 4.72−4.70 (m, 1H, CH, Is, H37), 2.94−2.81 (m,

3H, overlapping 2CH Duphos (H7/H10) and CH Is (H32)), 2.44−2.39 (m, 1H, CH Duphos, H19), 1.99−1.77 (m, 4H, $2CH_2$), 1.64−1.53 (m, 4H, CH_2), 1.49 (dd, J = 17, 7, 3H, CH_3 Duphos, H20), 1.39 (dd, J = 17, 10, 3H, CH_3 Duphos, H12), 1.36−1.29 (m, 7H, overlapping $2CH_3$ Is (H29/H38) and 1CH Duphos (H23)), 1.23 (broad d, J = 7, 9H, CH_3 Is, H39/H33/H34), 1.03 (d, J = 7, 3H, CH_3 Is, H28), 0.77−0.73 (m, 6H, overlapping CH_3 Duphos (H11) and P−Me (H40), J_{Pt-H} = 57), 0.61 (dd, J = 14, 7, 3H, CH_3 Duphos, H24). $^{13}C\{^1H\}$ NMR (−60 °C, THF-d_8): δ 163.0 (d, J = 95, J_{Pt-C} = 803, Pt−C (quat Ph, C1)), 155.6 (quat Is, C31), 154.0 (d, J = 26, P−C (quat Is, C25)), 148.1 (2 quat Is, C26/C36), 147.2−146.6 (m, quat Duphos, C18), 144.1−143.3 (m, quat Duphos, C13), 140.2 (d, J = 25, Ph *ortho*, C6), 137.9 (Ph ortho, *C*2), 135.2−134.6 (m, Ar, Duphos, C16), 134.5−134.0 (m, Ar, Duphos, C15), 131.9 (d, J = 25, Ar, Duphos, C17), 131.3 (d, J = 25, Ar, Duphos, C14), 128.3 (d, J = 30, Ph meta, C5), 128.1 (d, J = 32, Ph meta, C3), 122.1 (d, J = 16, Ph para, C4), 121.8 (d, J = 10, Is meta, C30), 120.0 (m, Is meta, C35), 45.1−44.7 (m, CH Duphos, C19), 42.4 (d, J = 32, CH Duphos, C10), 38.1 (broad, CH_2), 36.9−35.7 (broad, overlapping CH_2), 35.5 (d, J = 32, CH, Is, C32), 35.1 (d, J = 23, CH, Is, C37), 33.4 (d, J = 34, CH, Is, C27), 32.9 (d, J = 33, CH, Duphos, C7), 32.6 (d, J = 23, CH, Duphos, C23), 28.3 (CH_3, Is, C28), 28.1 (CH_3, Is, C39), 27.3 (CH_3, Is, C38), 25.1 (CH_3, Is, C33), 24.9 (CH_3, Is, C34), 22.3 (CH_3, Is, C29), 18.8−18.2 (m, CH_3, Duphos, C20), 16.3−15.9 (m, CH_3, Duphos, C12), 15.5 (d, J = 15, CH_3, Duphos, C24), 15.1 (d, J = 13, CH_3, Duphos, C11), 12.4 (broad, P−CH_3, C40).

Acknowledgment. We thank the National Science Foundation for support and Karen Goldberg (University of Washington) for a helpful suggestion.

Note Added after ASAP Publication. In the version of this paper published on the Web on February 20, 2007, the chemical formulas on the last line of the right-hand column on the second page of the paper were incorrect, due to a production error. The version that now appears is correct.

Supporting Information Available: Text, figures, and tables giving more experimental and characterization data, details of the X-ray structure determinations, and additional information on the NMR structure determination of complex **4** and CIF files giving crystal data. This information is available free of charge via the Internet at http://pubs.acs.org.

OM061116S